

A conformal test of linear models via permutation-augmented regressions

Leying Guan*

Abstract

Permutation tests are widely recognized as robust alternatives to tests based on normal theory. Random permutation tests have been frequently employed to assess the significance of variables in linear models. Despite their widespread use, existing random permutation tests lack finite-sample and assumption-free guarantees for controlling type I error in partial correlation tests. To address this ongoing challenge, we have developed a conformal test through permutation-augmented regressions, which we refer to as PALMRT. PALMRT not only achieves power competitive with conventional methods but also provides reliable control of type I errors at no more than 2α , given any targeted level α , for arbitrary fixed designs and error distributions. We have confirmed this through extensive simulations.

Compared to the cyclic permutation test (CPT) and residual permutation test (RPT), which also offer theoretical guarantees, PALMRT does not compromise as much on power or set stringent requirements on the sample size, making it suitable for diverse biomedical applications. We further illustrate the differences in a long-Covid study where PALMRT validated key findings previously identified using the t-test after multiple corrections, while both CPT and RPT suffered from a drastic loss of power and failed to identify any discoveries. We endorse PALMRT as a robust and practical hypothesis test in scientific research for its superior error control, power preservation, and simplicity. An R package for PALMRT is available at <https://github.com/LeyingGuan/PairedRegression>.

Key words: Partial correlation; Random permutation; Assumption-free; Conformal test.

*Dept. of Biostatistics, Yale University, leying.guan@yale.edu

1 Introduction

Consider a linear regression model

$$y_i = x_i\beta + \mathbf{z}_i^\top \theta + \epsilon_i, i = 1, \dots, n \quad (1)$$

with features $x_i \in \mathbb{R}$ and $\mathbf{z}_i \in \mathbb{R}^p$, and random errors ϵ_i independent of (x_i, \mathbf{z}_i) . Testing whether the coefficient β is zero in this linear model, or equivalently, examining the partial correlation between x and y , remains a fundamental statistical query and a prevalent approach in applications like biological signature discovery. For instance, a key question in the recent MY-LC study is whether long-COVID (LC) is associated with specific cell type proportions, after adjusting for age, sex, and Body Mass Index (BMI) (Klein et al., 2023) :

$$\text{cell type frequency} \sim \text{intercept} + \text{LC} + \text{age} + \text{sex} + \text{BMI} + \text{age} \times \text{BMI} + \text{sex} \times \text{BMI}. \quad (2)$$

While the F/t-test is a standard approach (Fisher, 1922; Fisher et al., 1924; Fisher, 1970), it may yield anti-conservative p-values under ill-behaved error distributions or limited sample sizes, compromising the reliability of scientific discoveries. Therefore, there is a need for a valid hypothesis test that minimizes assumptions on the noise distribution and does not rely on asymptotic theory. Motivated by this, we seek a robust and straightforward testing procedure for partial correlation under the sole assumption of exchangeability.

Assumption 1.1. *The noise variables $\epsilon_1, \dots, \epsilon_n$ are exchangeable with in law.*

The problem of testing partial correlations has been intensively studied, with a focus on developing various random permutation methods to increase robustness against diverse noise distributions. Draper and Stoneman (1966) introduced a permutation technique for partial correlation testing, referred to as PERMtest, which involves permuting x alone and disrupts the relationship between x and Z . Subsequent methods better accounted for this relationship. A family of methods, such as the Freedman and Lane test (FLtest) (Freedman and Lane, 1983) and the Kennedy-test (Kennedy, 1995), permutes response residuals obtained from a reduced model that regresses y on Z . Another type of method, such as the Braak-test (Ter Braak, 1992), shuffles residuals from a full model regressing y on both x and Z . These methods have demonstrated empirically robust type I error control in various benchmark studies when using pivotal test statistics like t-test or F-test statistics (Hall and Wilson, 1991; Westfall and Young, 1993; Anderson and Robinson, 2001; Winkler et al., 2014). However, finite-sample and assumption-free theoretical guarantees for

these random permutation tests remain elusive. This contrasts with permutation tests for simple correlation, which are theoretically sound in terms of type I error control (Pitman, 1937; Manly, 2006; Edgington and Onghena, 2007). Indeed, even the widely-examined and recommended FLtest can, under specific conditions, yield drastically inflated type I error rates, as we demonstrate later.

Recently, Lei and Bickel (2021) introduced the cyclic permutation test (CPT), which offers worst-case guarantees for controlling type I error. Given a sample size n and a total feature dimension p for z , CPT theoretically ensures type I error control at a target level α , provided $n > (\frac{1}{\alpha} - 1)p$. This condition is often challenging to meet in biomedical studies. For instance, in immunology research, sample sizes frequently hover around 100 or a few hundreds, while investigating simultaneously hundreds or even more different biomarkers for their partial correlations with a primary feature of interest. Although applying CPT with a $\alpha = 0.05$ cutoff may suffice with fewer concomitant covariates, the situation complicates when multiple hypothesis corrections are applied, as smaller nominal p -value thresholds are needed to maintain a reasonable false discovery rate (FDR). In an independent pursuit of robust partial correlation analysis with increased power and reduced sample size, Wen et al. (2022) introduces the residual permutation test (RPT), defined under the condition $n > 2p$. This test utilizes a sequence of specially-designed permutation matrices, which, in conjunction with the identity matrix, form a group. However, there’s a trade-off in the choice of the size parameter K : a small permutation set size limits testing for small p -values, while a large K reduces RPT power significantly by design (see Table 1). Obtaining a sequence of well-designed permutation matrices with a reasonable size, such as $(\lceil \frac{1}{\alpha} \rceil - 1)$ as suggested by Wen et al. (2022), remains challenging for small α . Following the proposed RPT Algorithm Wen et al. (2022), a non-trivial test requires $\alpha > \frac{1}{n}$.

In this manuscript, we develop PALMRT, which stands for Permutation-Augmented Linear Model Regression Test, as a conformal test to examine the partial correlation relationships in a linear model. Unlike traditional random permutation methods, PALMRT not only empirically controls type I error but also theoretically guarantees a worst-case coverage of 2α at any targeted error level α . It offers well-calibrated p -values for finite-sample type I error control under arbitrary fixed designs or noise distributions. Table 1 provides a brief summary of different methods regarding their construction, empirical performance, theoretical guarantee, and dimension constraints for non-trivial rejection under the i.i.d random Gaussian design.

In our empirical analyses, PALMRT not only maintains empirical Type I error rates below the designated thresholds across diverse simulation settings but also exhibits comparable power to established methods like FLtest when (n/p) is mod-

erately large. It significantly outperforms CPT and RPT in commonly encountered scenarios. Upon re-analyzing the MY-LC study, PALMRT validates the top findings from the original study, while CPT and RPT show reduced discoveries and fail to confirm any main findings after multiple test corrections. Consequently, we recommend adopting PALMRT as the default robust procedure for detecting significant partial correlations in our daily research.

In our empirical analyses, PALMRT not only maintains empirical Type I error rates below the designated thresholds across diverse simulation settings but also exhibits comparable power to established methods like FLtest when (n/p) is moderately large and outperforms CPT in commonly encountered scenarios. Upon re-analyzing the MY-LC study, we confirmed the robustness of the top findings from the original study using PALMRT. Consequently, we advocate for the adoption of PALMRT as a robust default procedure for detecting significant partial correlations in our daily research.

2 Conformal test via permutation-augmented regressions

2.1 Construction of PALMRT

Let $x \in \mathbb{R}^n$ be the target feature, and Z the observation matrix with rows $\mathbf{z}_1, \dots, \mathbf{z}_n$. Define $[n]$ as the vector $(1, \dots, n)$ and π as a permutation of $[n]$. Denote x_π and Z_π as the row-permuted versions of x and Z respectively. PALMRT is a random permutation method for testing partial correlation. For each randomly generated permutation π of $[n]$, it constructs “original” and “permuted test” statistics based on a pair of permutation-augmented regressions:

- Original test statistic $T_{original}$: the F-statistic for significance of x in the model $y \sim x + Z + Z_\pi$:

$$T_{original} = (\|(I - H^{zz_\pi})y\|_2^2 - \|(I - H^{xzz_\pi})y\|_2^2) / \|(I - H^{xzz_\pi})y\|_2^2.$$

- Permuted test statistic T_{perm} : the F-statistic for significance of x_π in the model $y \sim x_\pi + Z + Z_\pi$:

$$T_{perm} = (\|(I - H^{zz_\pi})y\|_2^2 - \|(I - H^{x_\pi zz_\pi})y\|_2^2) / \|(I - H^{x_\pi zz_\pi})y\|_2^2.$$

Here, H^* denotes the projection matrix onto the column space of its argument $*$. For instance, $H^{z_\pi z}$ represents the projection matrix onto the column space of (Z_π, Z) ,

Table 1: Summary of representative existing permutation methods and PALMRT. Let H^z and H^{xz} represent the projection matrices onto the column spaces of the concomitant features Z and all features (x, Z) , respectively. Given a permutation π of $(1, \dots, n)$, x_π and Z_π denote the permuted versions of x and Z . The intercept in the linear model is omitted for brevity. The columns labeled “Original Model” and “Permuted Model” detail the models used to generate the original and permuted test statistics, respectively. For CPT, η is a length- n vector used to define valid cyclic permutations and generate m cyclic permutation copies. Define $L = \lfloor \frac{n}{m} \rfloor$ as the cyclic step size. CPT requires $\eta^\top Z_{(kL+1):(kL+n)}$ to be a constant vector for all $0 \leq k \leq m$, where an index greater than n is looped back from the beginning, e.g., $x_{kL+n} = x_{kL}$. Let $V \in \mathbb{R}^{n \times (n-p)}$ be an orthonormal matrix orthogonal to the column space of Z . RPT generates m permutations π_1, \dots, π_m based on a variant of cyclic permutation to satisfy the group requirement, resulting in V_{π_k} as the row-permuted version of V for $k = 1, \dots, m$. RPT then constructs $\tilde{V}_k \in \mathbb{R}^{n \times (n-2p)}$ as the orthonormal matrix belonging to the intersection of the column space of V and V_{π_k} . The “Empirical” column indicates empirical type I error control from previous studies (statement on PALMRT is based on our study). The column “Worst-case” indicates the finite-sample and assumption-free theoretical guarantee for a given level α , and “ $\gg \alpha$ ” represents that no guarantee has been established. The column “Restriction” specifies the minimum sample size when a test is defined and can be non-trivial under an i.i.d Gaussian design. Except CPT and RPT, F-statistics are utilized for comparison.

Method	Original Model	Permuted Model	Empirical	Worst-Case	Restriction
PERMtest	$y \sim x + Z$	$y \sim x_\pi + Z$	$\lesssim \alpha$	$\gg \alpha$	$n > p$
FLtest	$y \sim x + Z$	$[(I - H^z)y]_\pi \sim x + Z$	$\lesssim \alpha$	$\gg \alpha$	$n > p$
Kenny-test	$y \sim x + Z$	$[(I - H^z)y]_\pi \sim (I - H^z)x$	$\lesssim \alpha$	$\gg \alpha$	$n > p$
Braak-test	$y \sim x + Z$	$H^{xz}y + [(I - H^{xz})y]_\pi \sim x + Z$	$\lesssim \alpha$	$\gg \alpha$	$n > p + 1$
CPT	$\eta^\top y$	$\eta^\top y_{(kL+1):(kL+n)}$	$\approx \alpha$	$\leq \alpha$	$\frac{n}{p} > \frac{1}{\alpha} - 1$
RPT	$\min_{\tilde{V} \in \{\tilde{V}_1, \dots, \tilde{V}_m\}} x^\top \tilde{V} \tilde{V}^\top y $	$ x^\top \tilde{V}_k \tilde{V}_k^\top y_{\pi_k} $	$\lesssim \alpha$	$\leq \alpha$	$n > \max(2p, \frac{1}{\alpha})$
PALMRT	$y \sim x + Z + Z_\pi$	$y \sim x_\pi + Z_\pi + Z$	$\lesssim \alpha$	$\leq 2\alpha$	$n > 2p$

$H^{xzz\pi}$ onto that of (x, Z, Z_π) , etc. We have more confidence of having non-zero β if $T_{original}$ is larger than T_{perm} . One can easily verify that comparing $T_{original}$ and T_{perm} is equivalent to comparing the following simplified expressions on the fitted residuals:

$$T_{original} = \|(I - H^{x\pi z z \pi})y\|_2^2, \quad T_{perm} = \|(I - H^{x z z \pi})y\|_2^2. \quad (3)$$

We adopt eq. (3) to construct the original and permuted statistics for any given permutation. Subsequently, we generate B random permutations $\{\pi_b\}_{b=1}^B$ of $[n]$ uniformly and compare the associated original and permuted statistics to compute the p-value for testing $H_0 : \beta = 0$. The complete procedure is outlined in Algorithm 1.

Algorithm 1 A conformal test for partial correlation via paired regression

- 1: **procedure** PALMRT(y, x, Z, B) ▷ Test for partial correlation $y \sim x|Z$ using B permutations
- 2: **for** $b = 1, \dots, B$ **do**
- 3: Generate a random permutation π_b .
- 4: Construct a pair of statistics as in eq. (3) with $\pi \leftarrow \pi_b$:

$$(T_{0b}, T_{b0}) \leftarrow (T_{original}, T_{perm})$$

- 5: Set $\omega_b = \frac{1}{2}\mathbb{1}\{T_{b0} = T_{0b}\} + \mathbb{1}\{T_{b0} > T_{0b}\}$.
 - 6: **end for**
 - 7: Construct p-value for $H_0 : \beta = 0$ as $p_{val} \leftarrow \frac{1 + \sum_{b=1}^B \omega_b}{B+1}$.
 - 8: **return** p_{val}
 - 9: **end procedure**
-

2.2 An example differentiating FLtest and PALMRT

We offer an illustrative example, see Example 2.1, to demonstrate PALMRT’s superior robustness compared to FLtest. Although FLtest has been lauded for its type I error control in prior studies, it may fail under extreme noise and design configurations. In contrast, PALMRT consistently maintains type I error control.

Example 2.1. We set $n = 100$ and $p = 1$, and examine a special design where $x = (1, 0, \dots, 0)^\top$, $z = (0, 1, 0, \dots, 0)^\top$. We generate the response y under the global null as $y \sim \varepsilon$, where $\varepsilon \sim N(0, I_{n \times n}) + 10^4 \times \text{Multinomial}(1; \frac{1}{n}, \dots, \frac{1}{n}) \times (-1)^{\text{Bernoulli}(\frac{1}{2})}$, denoted as “multinomial noise.” This extreme noise scenario serves as a robustness test. The feature design represents an imbalanced ANOVA setup with many control

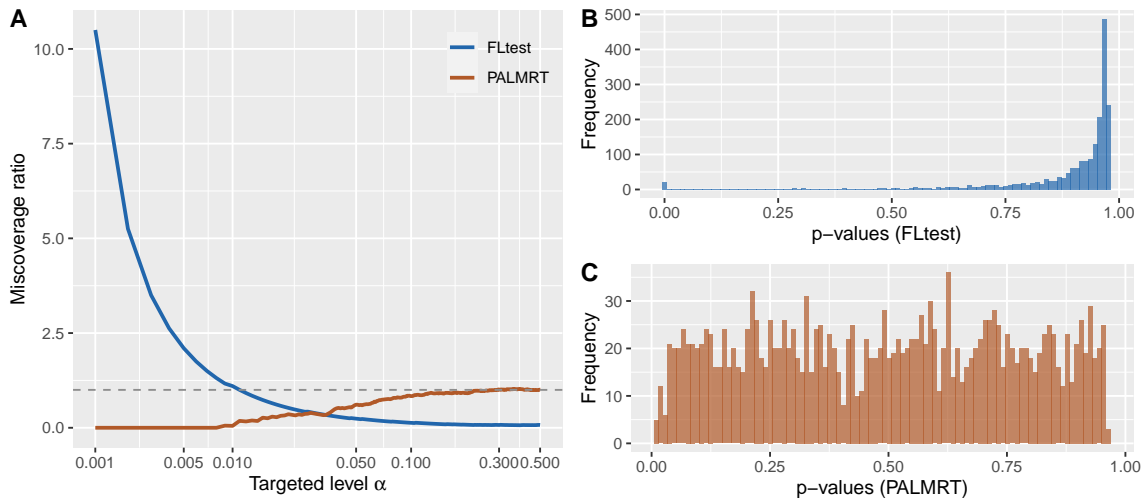


Figure 1: Comparison between FLtest and PALMRT on a distinguishing example. Panel A shows the miscoverage ratios using FLtest and PALMRT in Example 2.1 as we range α from 0.001 to 0.5. Panels B-C display the histograms of p-values using the two tests.

samples but only one sample per treatment group. Even though exact permutation is feasible by shuffling the zero rows, we employ standard FLtest and PALMRT to evaluate their empirical coverage using 2000 random draws of y . Figure 1A shows the miscoverage ratio, defined as

$$\text{miscoverage ratio} = \frac{\text{Empirical miscoverage}}{\text{Targeted miscoverage}}.$$

As the targeted level α becomes small, FLtest encountered excessively inflated type I error – more than 10-fold that of the targeted level when $\alpha = 0.001$. In contrast, PALMRT controls type I error for small α . Figures 1B-C are the histograms of p-values using FLtest and PALMRT. The distribution of p-values from FLtest contains a spike close to 0, leading to its type I error inflation.

Example 1 is a distinguishing example where FLtest suffers from being severely anti-conservative for small α but PALMRT continues to offer robust type I error control. This robustness of PALMRT is universally true. In the next section, we will show that PALMRT, as well as a family of other permutation tests based on paired constructions, guarantees a maximum type I error of 2α , irrespective of the noise distribution, design, and sample size.

3 Type I error control guarantee

In this section, we establish that PALMRT provides finite-sample type I error guarantees under any design and exchangeable noise. This property is generalized to a family of tests that performs comparisons with paired statistics as realizations of a specially-designed bi-variate function on permutation orders.

Under the null hypothesis H_0 , PALMRT essentially compares a bi-variate function across two given permutations and their swaps. Specifically, for any two permutations π_1 and π_2 of $[n]$, we define a bi-variate function, which also incorporates data x , Z , and unobserved noise ε as model parameters, as follows:

$$T^{PALMRT}(\pi_1, \pi_2; x, Z, \varepsilon) = \|(I - H^{x_{\pi_2} z_{\pi_2} z_{\pi_1}})\varepsilon\|_2^2. \quad (4)$$

Let π_0 be the identity permutation of $[n]$.

Proposition 3.1. *Under the null hypothesis H_0 , the statistic pair (T_{0b}, T_{b0}) are realizations of $T^{PALMRT}(\cdot, \cdot; x, Z, \varepsilon)$ evaluated at (π_0, π_b) and (π_b, π_0) respectively:*

$$(T_{0b}, T_{b0}) = (T^{PALMRT}(\pi_0, \pi_b), T^{PALMRT}(\pi_b, \pi_0)).$$

Many existing random permutation tests, including FLtest and PERMtest, can be expressed as realizations of such bi-variate functions. For example, construct bi-variate functions $T^{PERM}(\cdot)$ and $T^{FL}(\cdot)$ defined below,

$$T^{PERM}(\pi_1, \pi_2; x, Z, \varepsilon) = \frac{\|(I - H^z)\varepsilon\|_2^2 - \|(I - H^{x_{\pi_1} z})\varepsilon\|_2^2}{\|(I - H^{x_{\pi_1} z})\varepsilon\|_2^2 / (n - p - 2)},$$

$$T^{FL}(\pi_1, \pi_2; x, Z, \varepsilon) = \frac{\|(I - H^{z_{\pi_1}})(I - H^z)\varepsilon\|_2^2 - \|(I - H^{x_{\pi_1} z_{\pi_1}})(I - H^z)\varepsilon\|_2^2}{\|(I - H^{x_{\pi_1} z_{\pi_1}})(I - H^z)\varepsilon\|_2^2 / (n - p - 2)}.$$

Let T_0 denote the original statistic and $\{T_b\}_{b=1}^B$ represent B permuted test statistics. Under H_0 , it can be verified via direct calculation that (T_0, T_b) are realizations at (π_0, π_b) and (π_b, π_0) of $T^{PERM}(\cdot, \cdot; x, Z, \varepsilon)$ or $T^{FL}(\cdot, \cdot; x, Z, \varepsilon)$ for PERMtest and FLtest respectively, with the second argument in the bivariate functions being inactive.

What sets $T^{PALMRT}(\dots)$ apart and enables its theoretical guarantee? The crucial distinction between $T^{PALMRT}(\dots)$ and $T^{FL}(\dots)$ or $T^{PERM}(\dots)$ lies in the transferability of permutations from the noise parameter ε to its permutation arguments. This property holds uniquely for $T^{PALMRT}(\dots)$ across all noise realizations and designs. Let σ be an arbitrary permutation of $[n]$ and σ^{-1} its inverse, such that $\sigma \circ \sigma^{-1} = \sigma^{-1} \circ \sigma = \pi_0$ with \circ denoting composition. Then, any permutation of the parameters ε in $T^{PALMRT}(\dots)$ can be expressed equivalently as applying the inverse permutation σ^{-1} to the permutation arguments π_1 and π_2 .

Proposition 3.2. *The application of a permutation σ to ε is equivalent to applying the permutation σ^{-1} to π_1, π_2 in T^{PALMRT} :*

$$T^{PALMRT}(\pi_1, \pi_2; x, Z, \varepsilon_\sigma) = T^{PALMRT}(\pi_1 \circ \sigma^{-1}, \pi_2 \circ \sigma^{-1}; x, Z, \varepsilon).$$

Proposition 3.2 is derived from simple term rearrangement, and we omit its proof here. This transferability property is pivotal for establishing the type I error guarantees. In fact, for any paired statistics T_{0b}, T_{b0} which can be considered as realizations of a bi-variate function $T(\cdot, \cdot; x, Z, \varepsilon)$ at (π_0, π_b) and (π_b, π_0) under H_0 , the resulting p-value from comparing T_{0b} to T_{b0} offers a theoretical guarantee as long as $T(\cdot, \cdot; x, Z, \varepsilon)$ satisfies the transferability condition 3.1, as outlined in Theorem 3.3.

Condition 3.1. *For any permutations π_1, π_2, σ of $[n]$, the function $T(\cdot, \cdot; x, Z, \varepsilon)$ satisfies*

$$T(\pi_1, \pi_2; x, Z, \varepsilon_\sigma) = T(\pi_1 \circ \sigma^{-1}, \pi_2 \circ \sigma^{-1}; x, Z, \varepsilon).$$

Theorem 3.3. *Let π_1, \dots, π_B be B uniformly random permutations of $[n]$, and $T(\cdot, \cdot; x, Z, \varepsilon)$ be a bi-variate function satisfying condition 3.1. Under the null hypothesis H_0 , construct paired statistics (T_{0b}, T_{b0}) as*

$$T_{0b} = T(\pi_0, \pi_b; x, Z, \varepsilon), \quad T_{b0} = T(\pi_b, \pi_0; x, Z, \varepsilon).$$

Substituting these into Algorithm 1, we obtain $\mathbb{P}_{H_0}[p_{val} \leq \alpha] < 2\alpha$ for all $\alpha > 0$, where the probability is marginalized over both noise and permutation randomness.

Remark 3.4. *Interestingly, the empirical version of RPT, discussed independently in Wen et al. (2022), is also a realization of paired constructions described in Theorem 3.3 when $(Z_0, Z_{\pi_b^{-1}})$ is full rank for different permutations π_b , by setting*

$$T(\pi_1, \pi_2; x, Z, \varepsilon) = |x_{\pi_2^{-1}}(I - H^{z_{\pi_1^{-1}} z_{\pi_2^{-1}}})\varepsilon|.$$

This leads to the comparison between $T_{0b} = |x(I - H^{z z_{\pi_b^{-1}}})y|$ and $T_{b0} = |x_{\pi_b^{-1}}(I - H^{z z_{\pi_b^{-1}}})y|$, which can be easily verified. In Wen et al. (2022), the authors recognized the power issue with RPT and introduced this empirical version to enhance power. However, it lacks theoretical justification. Here, we demonstrate also that the empirical RPT has a strong theoretical foundation as a special case of Theorem 3.3 and is a version of PALMRT by replacing the pivotal statistics with residuals inner product, hence, the requirement on permutations by RPT is unnecessary in its context.

The worst-case bound established in Theorem 3.3 aligns with the bounds for prediction coverage established for multisplit conformal prediction methods including CV+, Jackknife+, and ensemble conformal predictions (Vovk et al., 2018; Barber et al., 2021; Kim et al., 2020; Gupta et al., 2022; Han et al., 2023). However, our focus diverges significantly as we concentrate on hypothesis testing for the true model parameter β rather than an out-of-sample prediction. Traditional exchangeability arguments, applicable when predicting on new samples, are inadequate for assessing the significance of β . To tackle this, we employ new arguments exploiting the assumption of exchangeable noise. A proof sketch for Theorem 3.3 is provided below.

Proof sketch of Theorem 3.3. One key insight is that, when considering both the randomness in the permutations and ε , the $(B + 1) \times (B + 1)$ matrix T , with its (l, k) -th entry as $T(\pi_l, \pi_k; x, Z, \varepsilon)$, is distributionally equivalent to \tilde{T} whose (l, k) -th entry is $T(\tilde{\pi}_l, \tilde{\pi}_k; x, Z, \varepsilon)$ with $(\tilde{\pi}_l)_{l=0}^B$ independently and uniformly generated from the permutation space of $[n]$. This equivalence allows us to analyze the p-value from Algorithm 1 by examining corresponding entries in \tilde{T} .

Define $f(l, \tilde{T}) = 1 + \sum_{k \neq l} \left(\mathbb{1}\{\tilde{T}_{kl} > \tilde{T}_{lk}\} + \frac{1}{2} \mathbb{1}\{\tilde{T}_{kl} = \tilde{T}_{lk}\} \right)$. Then, $f(0, \tilde{T})$ corresponds to the numerator when constructing p_{val} , the p-value in Algorithm 1, upon substituting T with \tilde{T} . Since $\tilde{\pi}_l$ are i.i.d. generated, we expect $\{f(l, \tilde{T})\}_{l=0}^B$ to be exchangeable for different l . Thus, we can bound $p_{val} \leq \alpha$ by bounding the size of the index set $\{l : f(l, \tilde{T}) \leq \alpha(B + 1)\}$, which can be obtained following similar arguments used in proving prediction interval's coverage for multi-split conformal prediction. \square

Theorem 3.3 is the main theoretical result of this work, and we include its full proof in Section 5. Combining Theorem 3.3 with Proposition 3.2, we conclude that Algorithm 1 theoretically controls type I error, albeit with a relaxed upper bound of 2α .

Of note, unlike existing random permutation tests where the use of pivotal statistics is often crucial, Theorem 3.3 generalizes beyond pivotal statistics, allowing for other non-pivotal paired constructions. For example, T_{0b}, T_{b0} could be the absolute value of the regression coefficients of x and x_π in the models $y \sim x + Z + Z_{\pi_b}$ and $y \sim x_\pi + Z + Z_{\pi_b}$ respectively. For directional tests, the test statistics may employ either the regression coefficients (for positive effects) or their negations (for negative effects).

4 An Exact Confidence Interval Construction

In conjunction with the PALMRT p -value, a confidence interval for β can be constructed by inverting the test. Define $(T_{0b}(\beta), T_{b0}(\beta))$ as the test statistics from replacing y by $(y - x\beta)$ in Algorithm 2 when constructing (T_{0b}, T_{b0}) . Define $f(\beta)$ as $f(\beta) = \frac{1 + \sum_{b=1}^B \omega_b(\beta)}{B+1}$, where $\omega_b(\beta) = \mathbb{1}\{T_{0b}(\beta) < T_{b0}(\beta)\} + \frac{1}{2}\mathbb{1}\{T_{0b}(\beta) = T_{b0}(\beta)\}$.

Corollary 4.1. *Set $CI_\alpha = [\beta_{\min}, \beta_{\max}]$ where $\beta_{\min} = \inf\{\beta : f(\beta) > \alpha\}$ and $\beta_{\max} = \sup\{\beta : f(\beta) > \alpha\}$. Then, we have $\min_\beta \mathbb{P}[\beta \in CI_\alpha] > 1 - 2\alpha$, for all $\alpha > 0$.*

Remark 4.2. *The set obtained through directly inverting $\{\beta : f(\beta) > \alpha\}$, is often an interval, but not always guaranteed to be so. By taking the infimum and supremum of this set, we obtain a confidence interval CI_α with worst-case guarantee at least as strong as direct inversion.*

The pertinent question remaining is the efficient computation of the confidence interval CI_α as delineated in Corollary 4.1. Traditional methods for constructing the confidence interval in permutation tests typically rely on normal theory, Bootstrap (Efron, 1987; Efron and Tibshirani, 1994; DiCiccio and Efron, 1996; Davison and Hinkley, 1997), or grid search (Garthwaite, 1996). Here, we provide an exact formulation of CI_α via examining critical values, derived from pair-wise comparisons at each permutation π_b . First, we observe that the contribution from the b^{th} term to the numerator is explicitly known.

Lemma 4.3. *Set $c_{b1} = \|(I - H^{x_{\pi_b} z_{\pi_b} z})x\|_2^2$, $c_{b2} = x^\top (I - H^{x_{\pi_b} z_{\pi_b} z})y$, $c_{b3} = \|(I - H^{x_{\pi_b} z_{\pi_b} z})y\|_2^2$, and $c_{b4} = \|(I - H^{x_{\pi} z_{\pi_b} z})y\|_2^2$. Then, we have $c_{b2}^2 \geq c_{b1}(c_{b3} - c_{b4})$ and*

$$\omega_b(\beta) = \begin{cases} \frac{1}{2}\mathbb{1}\{c_{b3} = c_{b4}\} + \mathbb{1}\{c_{b3} < c_{b4}\}, & \text{if } c_{b1} = 0, \\ \frac{1}{2}\mathbb{1}\{\beta \in [s_b, u_b]\} + \mathbb{1}\{\beta \in (s_b, u_b)\}, & \text{if } c_{b1} > 0, \end{cases} \quad (5)$$

where $s_b = \frac{c_{b2} - \sqrt{c_{b2}^2 - c_{b1}(c_{b3} - c_{b4})}}{c_{b1}}$ and $u_b = \frac{c_{b2} + \sqrt{c_{b2}^2 - c_{b1}(c_{b3} - c_{b4})}}{c_{b1}}$.

As a result, we first partition of index set of $\{0, \dots, B\}$ into three sets $A_1 = \{b : c_{b1} > 0\}$, $A_2 = \{b : c_{b1} = 0, c_{b3} < c_{b4}\}$, and $A_3 = \{b : c_{b1} = 0, c_{b3} = c_{b4}\}$. The value of $\omega_b(\beta)$ remains constant as we vary β for $b \in A_2 \cup A_3$. Hence, the requirement of $f(\beta) > \alpha$ is equivalent to imposing a requirement on $f_{A_1}(\beta)$ that captures the contribution of $\omega_b(\beta) \in A_1$, as shown below:

$$f(\beta) > \alpha \Leftrightarrow f_{A_1}(\beta) = \sum_{b \in A_1} \omega_b(\beta) > (B+1)\alpha - 1 - |A_2| - \frac{1}{2}|A_3| := \gamma.$$

It can be shown that the function value of $f_{A_1}(\beta)$ is characterized by comparing β to different s_b/u_b values for $b \in A_1$:

$$f_{A_1}(\beta) = \frac{1}{2}\#\{b : s_b \leq \beta\} + \frac{1}{2}\#\{b : s_b < \beta\} - \frac{1}{2}\#\{b : u_b \leq \beta\} - \frac{1}{2}\#\{b : u_b < \beta\}. \quad (6)$$

Let $t_1 < \dots < t_M$ denote the ordered values of M unique elements in $\cup_{b \in A_1} \{s_b, u_b\}$, and let (m_i^s, m_i^u) represent the sizes of $\#\{b : s_b = t_i\}$ and $\#\{b : u_b = t_i\}$, respectively. As we increase β in $f_{A_1}(\beta)$, the function value can only change when we first hit $\{t_i\}_{i=1}^M$, or when β slightly increases from these critical values represented. We represent the concept of increasing slightly from these critical values by $\{t_i^+\}_{i=1}^M$, where t_i^+ indicates being infinitesimally larger than t_i . Using these new quantities introduced, we can re-express $f_{A_1}(t_1) = \frac{1}{2}(m_1^s - m_1^u)$ and identify induction relations for the function values as we increase β to surpass the critical values t_i , described as follows:

$$f_{A_1}(t_{i+1}) = f_{A_1}(t_i^+) + \frac{1}{2}(m_{i+1}^s - m_{i+1}^u), \quad f_{A_1}(t_i^+) = f_{A_1}(t_i) + \frac{1}{2}(m_i^s - m_i^u). \quad (7)$$

We can utilize eq. (7) to efficiently calculate all $f_A(t_i)$ and $f_A(t_i^+)$ in $O(B)$ time, given $\{t_i\}_{i=1}^M$ and $(m_i^s, m_i^u)_{i=1}^M$. Acquisition of the $B \times 4$ matrix (c_{bl}) , $\{t_i\}_{i=1}^M$ and $(m_i^s, m_i^u)_{i=1}^M$ can be done in $O(Bnp + B \log B)$ time if we record intermediate quantities from Algorithm 1. Consequently, efficient comparisons between $f_A(\cdot)$ with γ to determine β_{\min} and β_{\max} can be achieved. Algorithm 2 presents full details of this implementation, and provides exact construction of CI_α as stated in Theorem 4.4.

Theorem 4.4. *The confidence interval constructed by Algorithm 2 corresponds to the CI_α defined in Lemma 4.1, and guarantees a worst-case coverage of $(1 - 2\alpha)$ for a specified mis-coverage level α .*

Remark 4.5. *The confidence interval CI_α can potentially be an empty set (\emptyset). Although this does not invalidate our assertion, an empty set offers limited information in practical contexts and might not be desired. In such situations, we may opt to construct the confidence interval using a normal approximation in the regression $y \sim x + Z$ whenever Algorithm 2 produces an empty set as the output for CI_α .*

Proofs of Lemma 4.3 and Theorem 4.4 are deferred to Appendix A in the Supplement.

5 Proof of Theorem 3.3

Before conducting numerical experiments comparing PALMRT and existing methods, we provide the full proof to Theorem 3.3 in this section. We define \mathcal{S}_n as the

Algorithm 2 Exact CI construction for PALMRT

1: **procedure** $\text{CI}(y, x, Z, B, \alpha)$ \triangleright Confidence interval at coverage level $1 - \alpha$.
2: Calculate the $B \times 4$ matrix $(c_{b1}, c_{b2}, c_{b3}, c_{b4})_{b=1}^B$ as defined in Lemma 4.3.
3: Calculate $\gamma, \{t_l\}_{l=1}^M, (m_l^s, m_l^u)_{l=1}^M$.
4: **if** $\gamma < 0$ **then**
5: $\text{CI}_\alpha = (-\infty, \infty)$.
6: **else**
7: Set and record $f_{A_1}(t_1) = \frac{1}{2}(m_1^s - m_1^u)$.
8: **for** $l = 2, \dots, M$ **do**
9: Calculate and record $f_{A_1}(t_{l-1}^+)$ and $f_{A_1}(t_l)$ as in eq. (7).
10: **end for**
11: **if** $\max(f_{A_1}(\cdot)) \leq \gamma$ **then**
12: $\text{CI}_\alpha = \emptyset$.
13: **else**
14: $\beta_{min} = \min\{t_l : f_{A_1}(t_l) \vee f_{A_1}(t_l^+) > \gamma\}$.
15: $\beta_{max} = \max\{t_l : f_{A_1}(t_l) \vee f_{A_1}(t_{l-1}^+) > \gamma\}$.
16: $\text{CI}_\alpha = [\beta_{min}, \beta_{max}]$.
17: **end if**
18: **end if**
19: **end procedure**

permutation space of $[n]$, \mathcal{S}_B as the permutation space of $(0, \dots, B)$, $\mathcal{E} = \{\varepsilon_1, \dots, \varepsilon_n\}$ as the unordered value set of $(\varepsilon_1, \dots, \varepsilon_n)$ (duplicates are allowed). Proposition 5.1 is useful for establishing our exchangeability statement. Proposition 5.2 is a minor modification of arguments for bounding “strange set” used in proving multi-splitting conformal prediction.

Proposition 5.1. *Let σ and $(\pi_b)_{b=1}^B$ be generated independently and uniformly from \mathcal{S}_n . Then σ^{-1} and $(\pi_b \circ \sigma^{-1})_{b=1}^B$ are also generated independently and uniformly from \mathcal{S}_n .*

Proof. First, it is obvious that σ^{-1} is uniformly generated from since the map $\sigma \mapsto \sigma^{-1}$ is a bijection between \mathcal{S}_n and itself. Hence, by definition, for any $(B + 1)$ permutations $\tau_0, \tau_1, \dots, \tau_B$ of $[n]$, we have

$$\begin{aligned} & \mathbb{P}(\sigma^{-1} = \tau_0, \pi_1 \circ \sigma^{-1} = \tau_1, \dots, \pi_B \circ \sigma^{-1} = \tau_B) \\ &= \mathbb{P}(\sigma^{-1} = \tau_0, \pi_1 = \tau_1 \circ \tau_0, \dots, \pi_B = \tau_B \circ \tau_0) \\ &= \mathbb{P}(\sigma^{-1} = \tau_0) \mathbb{P}(\pi_1 = \tau_1 \circ \tau_0) \dots \mathbb{P}(\pi_B = \tau_B \circ \tau_0) \\ &= (1/n!)^{B+1}, \end{aligned} \tag{8}$$

where the last two steps have used the fact that σ^{-1} and $(\pi_b)_{b=1}^B$ are independent and uniformly from \mathcal{S}_n . Eq (8) is the definition for σ^{-1} and $(\pi_b \circ \sigma^{-1})_{b=1}^B$ being independent and uniformly generated from \mathcal{S}_n . \square

Proposition 5.2. *Let T be any $(B+1) \times (B+1)$ matrix, and W the $(B+1) \times (B+1)$ comparison matrix where $W_{lk} = \mathbb{1}\{T_{kl} > T_{lk}\} + \frac{1}{2}\mathbb{1}\{T_{kl} = T_{lk}\}$ for $l \neq k$ and $W_{ll} = 1$. Let W_l be the l^{th} row sum of W . Then, for all $\alpha > 0$, we have*

$$|\{l : W_l \leq (B + 1)\alpha\}| < 2\alpha(B + 1).$$

Proof. Notice that (1) $W_{lk} \geq 0$ for all l, k , and (2) $W_{lk} + W_{kl} = 1$ for all $k \neq l$. For any sub-square matrix of W constructed from selecting the same m columns and rows (denoted the index set as I_m), we have

$$\sum_{l \in I_m} \sum_{k \in I_m} W_{lk} = \frac{(m + 1)m}{2}.$$

Set $S_\alpha = \{l : W_l \leq (B + 1)\alpha\}$. Suppose the size of S_α is $s \geq 0$. The corresponding s rows in W must implicate:

$$s\alpha(B + 1) \geq \frac{s(s + 1)}{2} \Rightarrow 0 \leq s \leq \max(0, 2\alpha(B + 1) - 1) < 2\alpha(B + 1).$$

This concludes our proof. \square

5.1 Proof to Theorem 3.3

On the one hand, under Assumption 1.1 and conditional on the value sets $\mathcal{E} = \{\varepsilon_1, \dots, \varepsilon_n\}$, generation of $(\pi_1, \dots, \pi_B, \varepsilon_\sigma)$ can be characterized by generating $\sigma, \pi_1, \dots, \pi_B, \sigma$ independently and uniformly generated from \mathcal{S}_n .

On the other hand, by Condition 3.1 and denoting π_0 as the identity permutation of $[n]$, we have

$$\begin{aligned} & (T(\pi_0, \pi_1; \varepsilon_\sigma), \dots, T(\pi_0, \pi_B; \varepsilon_\sigma), T(\pi_1, \pi_0; \varepsilon_\sigma), \dots, T(\pi_B, \pi_0; \varepsilon_\sigma)) \\ &= (T(\sigma^{-1}, \pi_1 \circ \sigma^{-1}; \varepsilon), \dots, T(\sigma^{-1}, \pi_B \circ \sigma^{-1}; \varepsilon), T(\pi_1 \circ \sigma^{-1}, \sigma^{-1}; \varepsilon), \dots, T(\pi_B \circ \sigma^{-1}, \sigma^{-1}; \varepsilon)). \end{aligned} \quad (9)$$

Here, we have dropped the parameters x and Z in $T(\cdot, \cdot; x, Z, \varepsilon)$ for convenience.

Write $\tilde{\pi}_0 = \sigma^{-1}$, $\tilde{\pi}_1 = \pi_1 \circ \sigma^{-1}$, \dots , $\tilde{\pi}_B = \pi_B \circ \sigma^{-1}$, by eq. (9) and Proposition 5.1, the marginalized joint distribution of the B pairs of statistics conditional only on \mathcal{E} can be re-expressed equivalently (in distribution) using $(\tilde{\pi}_b)_{b=1}^B$:

$$(T_{0b}, T_{b0})_{b=1}^B \stackrel{d}{=} (T(\tilde{\pi}_0, \tilde{\pi}_b; \varepsilon), T(\tilde{\pi}_b, \tilde{\pi}_0; \varepsilon))_{b=1}^B, \quad (10)$$

where $\tilde{\pi}_0, \dots, \tilde{\pi}_B$ are independently and uniformly generated from \mathcal{S}_n , and ε can be viewed as fixed. Hence, setting $(\tilde{T}_{0b}, \tilde{T}_{b0}) = (T(\tilde{\pi}_0, \tilde{\pi}_b; \varepsilon), T(\tilde{\pi}_b, \tilde{\pi}_0; \varepsilon))$, to understand the behavior of the constructed p-value using $(T_{0b}, T_{b0})_{b=1}^B$, we can equivalently consider the distribution of $\widetilde{\text{pval}}$:

$$\widetilde{\text{pval}} = \frac{1 + \sum_{b=1}^B \left(\mathbb{1}\{\tilde{T}_{b0} > \tilde{T}_{0b}\} + \frac{1}{2} \mathbb{1}\{\tilde{T}_{b0} = \tilde{T}_{0b}\} \right)}{B + 1}.$$

Now, we complete the full \tilde{T} matrix by setting $\tilde{T}_{kl} = T(\tilde{\pi}_k, \tilde{\pi}_l; \varepsilon)$ for all $k, l = 0, \dots, B$. We also set the comparison W matrix of \tilde{T} as described in Proposition 5.2 and set $S_\alpha = \{l : W_l \leq \alpha(B + 1)\}$. Then, by Proposition 5.2, the size of S_α is upper bounded and $|S_\alpha| < 2\alpha(B + 1)$.

Note that the p-value constructed using \tilde{T} is

$$\widetilde{\text{pval}} = \frac{1 + \sum_{b=1}^B \left(\mathbb{1}\{\tilde{T}_{b0} > \tilde{T}_{0b}\} + \frac{1}{2} \mathbb{1}\{\tilde{T}_{b0} = \tilde{T}_{0b}\} \right)}{B + 1} = \frac{W_0}{B + 1}.$$

To avoid confusion, we use the lower case $(w_b)_{b=1}^B$ to denote the observed row sums $(W_b)_{b=1}^B$ given the current realizations $(\tilde{\pi}_0, \dots, \tilde{\pi}_B) = (\tau_0, \dots, \tau_B)$, and $(W_b)_{b=1}^B$ be the random variables as we change the permutations $(\tilde{\pi}_0, \dots, \tilde{\pi}_B)$. Then, conditional on the unordered set of permutations $\{\tilde{\pi}_0, \dots, \tilde{\pi}_B\} = \{\tau_0, \dots, \tau_B\}$, the observed

permutations take the form $\tilde{\pi}_b = \tau_{\zeta_b}$, for $b = 0, \dots, B$, where ζ is a permutation of $(0, \dots, B)$. Since $\tilde{\pi}_0, \dots, \tilde{\pi}_B$ are i.i.d generated from \mathcal{S}_n , ζ is uniformly generated from the \mathcal{S}_B .

The above results can be used to derive the exchangeability among W_0, \dots, W_B conditional on \mathcal{E} and $\{\tilde{\pi}_0, \dots, \tilde{\pi}_B\} = \{\tau_0, \dots, \tau_B\}$. Notice that when $\tilde{\pi} = \tau_\zeta$ is permuted according to ζ , the row sum $W_0 = w_{\zeta_0}$ is permuted accordingly:

$$\begin{aligned} W_0 &= 1 + \sum_{b=1}^B \left(\mathbb{1}\{T(\tau_{\zeta_b}, \tau_{\zeta_0}; \varepsilon) > T(\tau_{\zeta_0}, \tau_{\zeta_b}; \varepsilon)\} + \frac{1}{2} \mathbb{1}\{T(\tau_{\zeta_b}, \tau_{\zeta_0}; \varepsilon) = T(\tau_{\zeta_0}, \tau_{\zeta_b}; \varepsilon)\} \right) \\ &= 1 + \sum_{b=1}^B \left(\mathbb{1}\{T_{\zeta_b, \zeta_0} > T_{\zeta_0, \zeta_b}\} + \frac{1}{2} \mathbb{1}\{T_{\zeta_b, \zeta_0} = T_{\zeta_0, \zeta_b}\} \right) \\ &= 1 + \sum_{b \neq \zeta_0} \left(\mathbb{1}\{T_{b, \zeta_0} > T_{\zeta_0, b}\} + \frac{1}{2} \mathbb{1}\{T_{b, \zeta_0} = T_{\zeta_0, b}\} \right) \\ &= w_{\zeta_0}. \end{aligned}$$

Combining the above display with the fact that ζ is uniform from \mathcal{S}_B , we conclude that $\{W_b\}_{b=0}^B$ are exchangeable. Consequently, we have

$$\mathbb{P}(W_0 \in S_\alpha) < 2\alpha \Rightarrow \mathbb{P}(\widetilde{p}_{\text{val}} \leq \alpha) < 2\alpha.$$

6 Numerical Experiments

We evaluate the performance and type I error control of various methods through numerical experiments, setting the sample size at $n = 100$, and varying the dimension of Z in $\{1, 5, 15\}$. We investigate four designs: i.i.d Gaussian, i.i.d Cauchy, balanced ANOVA where each feature takes roughly an equal number of non-overlapping 1s, and a paired design where each feature assumes a value of 1 at two entries and 0 elsewhere, with one unique and one shared one-valued entry across all features. We also consider three noise settings: Gaussian, Cauchy, and multinomial. The paired design and multinomial noise distributions are atypical in real-world applications and are included as challenging test cases for evaluating the robustness of FLtest, which has demonstrated commendable empirical performance under more conventional design structures and noise distributions in existing literature.

We compare our proposed PALMRT against six existing methods: (1) F-test, (2) PERMtest, (3) FLtest, (4) CPT with strong pre-ordering by the genetic algorithm as per Lei and Bickel (2021), (5) RPT, and (6) Bias-corrected and Accelerated Bootstrap, previously favored over plain Bootstrap (Efron, 1987; Diccio and Romano,

1988; Hall, 1988; DiCiccio and Efron, 1996). All comparisons were conducted at the p-value cut-off $\alpha = 0.05$ in the main paper; PALMRT’s type I error control is further explored for $\alpha = 0.01$ and $\alpha = 0.001$ in supplementary materials.

For random permutation tests (PALMRT, FLtest, PERMtest), we employed F-statistics as the test statistics and set the permutation count $B = 2000$. Bias-corrected and Accelerated Bootstrap and CPT can be more time-intensive. We used *bcaboot* R package with 500 bootstraps and 20 jackknife blocks (Efron and Narasimhan, 2020). For CPT, we used the implementation from the authors’ GitHub, followed the strong ordering approach with 10,000 optimization steps via genetic algorithms, and set the number of cyclic permutations as 19 (corresponding to $\alpha = 0.05$) (Lei and Bickel, 2021). For RPT, we used the implementation provided by the authors and set the the number of permutation as 19 (corresponding to $\alpha = 0.05$) as recommended (Wen et al., 2022).

We generated 2,000 independent noise instances ε for each experimental setting and used them to compute empirical type I error, statistical power, and confidence intervals across various signal-to-noise ratios. Sections 6.1 and 6.2 compare type I error and power among F-test, PERMtest, FLtest, CPT, RPT, and PALMRT. Section 6.3 examines CI coverage for β and their median lengths from independent runs using normal theory, Bootstrap and Algorithm 2.

6.1 Type I error control

To empirically assess type I error control, we simulate the global null distribution with $y = \varepsilon$. Figure 2 displays type I errors from 50 independent repetitions for each setting using F-test, PERMtest, FLtest, CPT, RPT and PALMRT.

In the Gaussian noise or the Gaussian/Cauchy design contexts, all methods effectively control type I errors. However, for ANOVA or Paired designs, Ftest, FLtest, and PERMtest yield inflated type I errors when noise is non-Gaussian – especially pronounced in the Paired design with multinomial errors. This underscores that not only F-test, but also FLtest and PERMtest, lack distribution-free theoretical guarantees and can be anti-conservative in finite-sample settings.

Among the methods tested, only PALMRT, CPT and RPT guarantee worst-case coverage across all experimental settings. Although CPT’s accurate type I error control is by design for $n/p \geq 19$, its accuracy in other settings was somewhat unexpected. For example, in the Gaussian design where $p = 15$, the cyclic invariant constraints of CPT can only be satisfied by a constant vector η with high probability, leading to a trivial test that always accepts H_0 . Further examination indicates that these observations arise because cyclic-invariant constraints of CPT

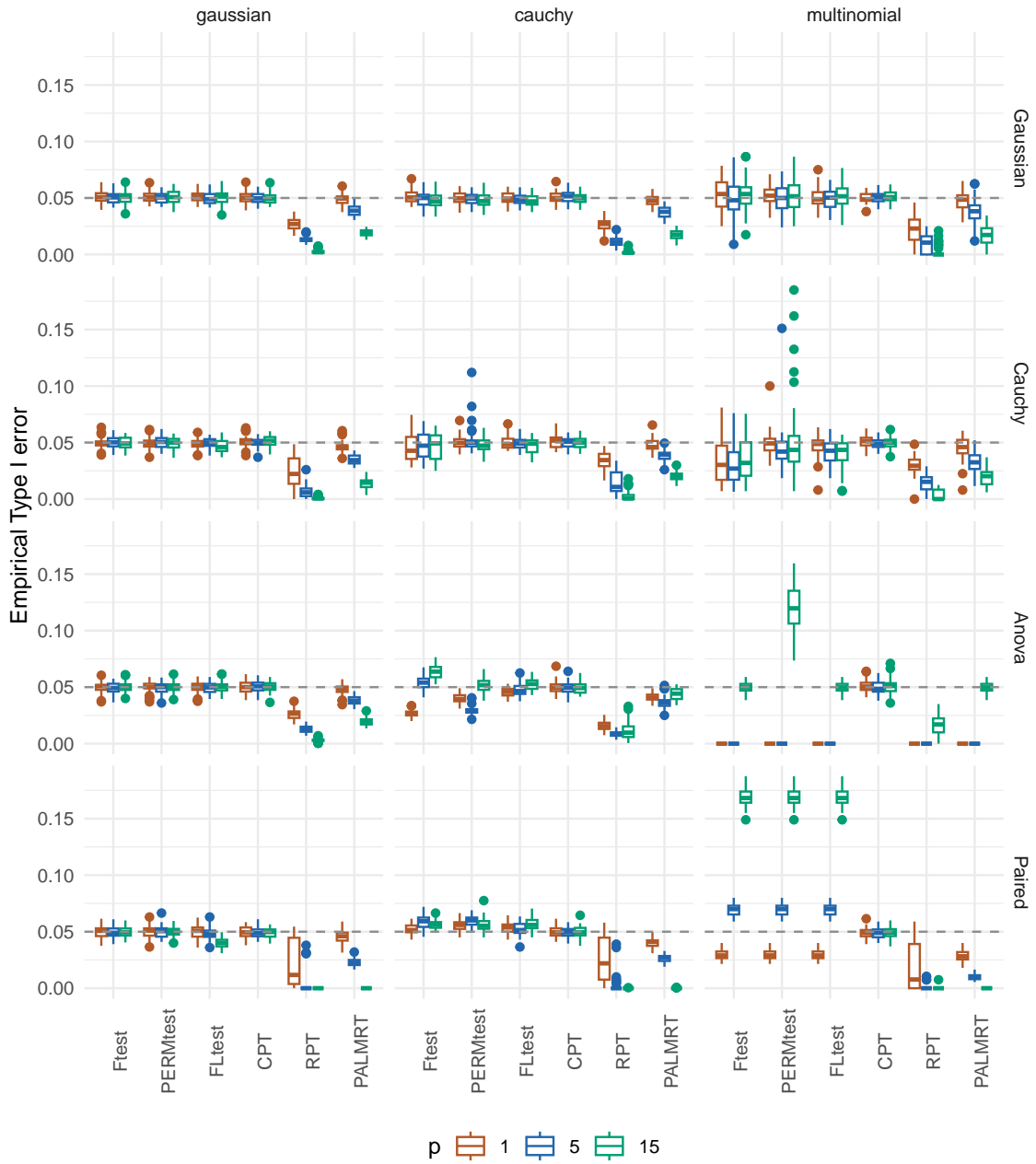


Figure 2: Empirical type I error using various methods, organized into boxplots by corresponding designs (row names) and noise distributions (column names). Each boxplot displays the empirical type I error for different methods, separately for different feature dimension p (color). The dashed horizontal line represents the targeted type I error $\alpha = 0.05$.

are not perfectly satisfied in the implemented CPT, thereby permitting non-constant η . PALMRT demonstrates empirical type I errors close to or below target levels, while RPT, as noted in its original paper, tends to be conservative, with the degree of conservativeness varying based on design, noise distribution, and dimensionality. Importantly, the conservative behavior of PALMRT does not sacrifice statistical power when compared to CPT and is generally more powerful compared to RPT, as evidenced by our subsequent power analyses.

6.2 Power Analysis

In each experiment, we simulate data from the alternative setting by varying the linear coefficient in front of x in eq. (11):

$$y = x\beta + \varepsilon. \tag{11}$$

We set β using Monte-Carlo simulation to yield F-test powers of approximately 30%, 50%, 70%, 90%, 99%. Figures 3-5 display the median of relative power of PALMRT to F-test, PERMtest, FLtest, CPT and RPT for varying signal strengths, noise distributions and feature dimensions under Gaussian, Cauchy, and ANOVA designs. For visualization purposes, if a median ratio is greater than 20, it is truncated at 20.

Under the Gaussian design, Ftest, PERMtest, and FLtest are most powerful across various noise types and feature dimensions. PALMRT closely rivals them at $p = 1$ and its relative sensitivity to low signal strength decreases with increased feature dimensions. PALMRT achieves higher power than CPT at $p = 1$ and substantially outperforms CPT at $p = 5$ and $p = 15$, despite being more empirically conservative for controlling the type I error. The gap between CPT and PALMRT does not disappear for $p = 5$ and $p = 15$ as we increase the signal strength. This is very different from the group bound method (Meinshausen, 2015) which is also conservative but is powerless compared to CPT in a wide range of signal-to-noise ratios when examined in Lei and Bickel (2021). PALMRT also shows much higher power compared to RPT with different concomitant feature dimension p , especially among the regime with a low signal-to-noise ratio.

In the Cauchy design, the relative sensitivities of PALMRT trend similarly to the Gaussian setting. However, F-test loses power with heavy-tailed noise distributions like Cauchy or multinomial, and random permutation tests can outperform F-test at low signal strengths. In the ANOVA design, results align with the Cauchy design when the noise is Gaussian or Cauchy. When the noise is multinomial, although the overall pattern is difficult to characterize, CPT and RPT are both significantly worse than PALMRT.

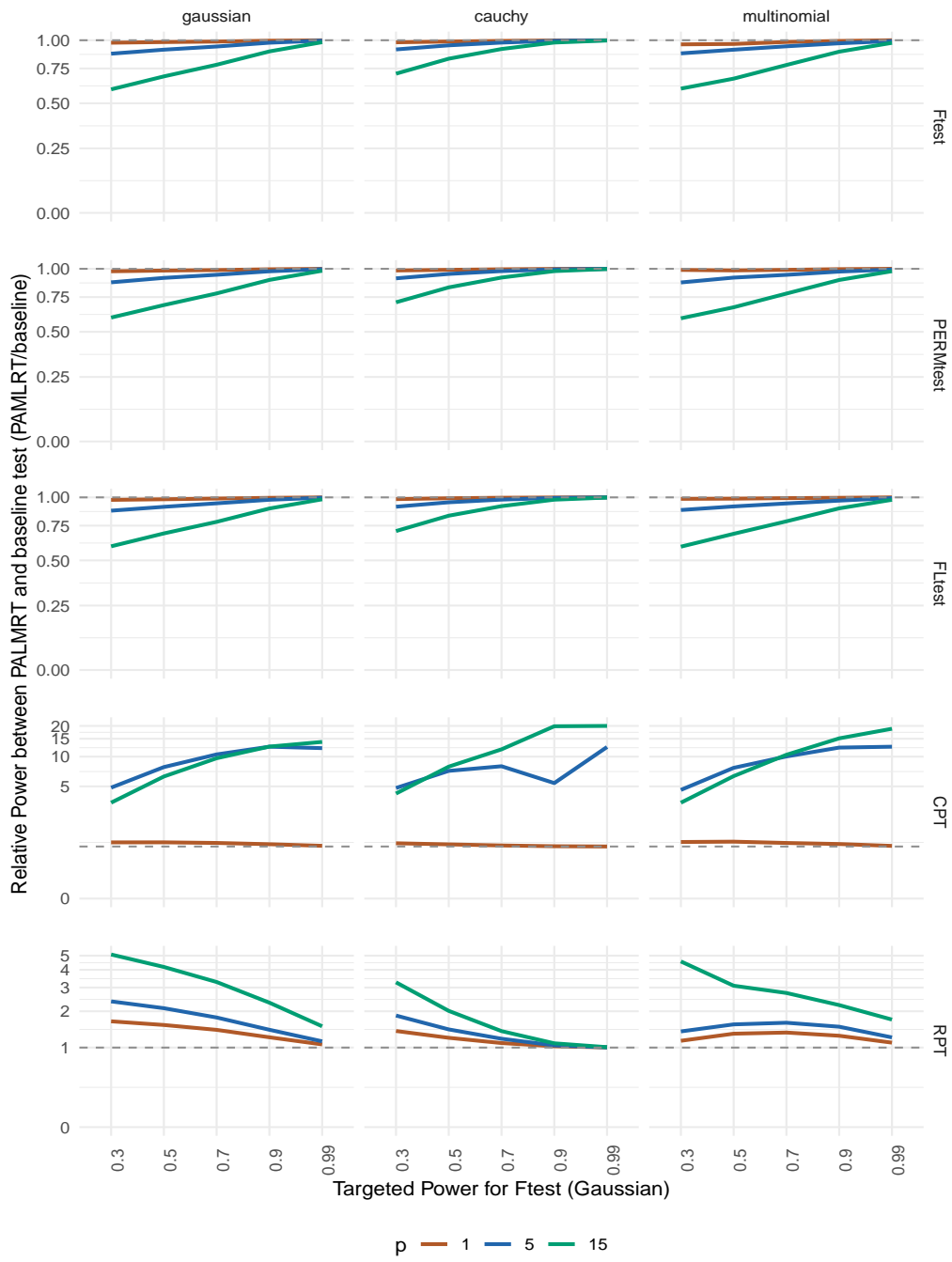


Figure 3: Power analysis in Gaussian design, presented as line plots, organized by baseline methods (row names) and noise distributions (column names). Each line plot shows the median power ratio between PALMRT and a baseline method, plotted against the targeted F-test absolute power for various signal sizes. Different colors indicate varying feature dimensions p .

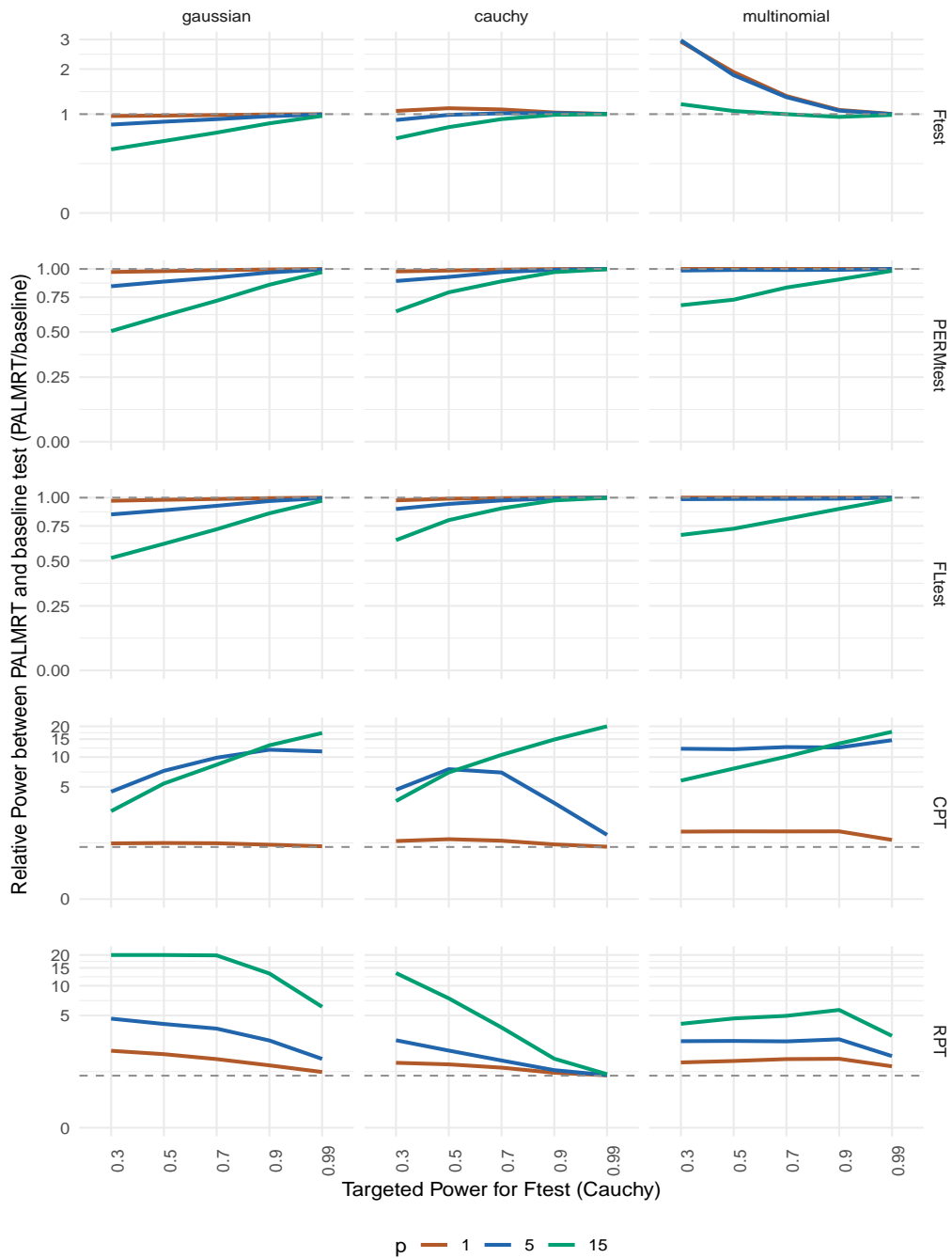


Figure 4: Power analysis in Cauchy design, presented as line plots, organized by baseline methods (row names) and noise distributions (column names). Each line plot shows the median power ratio between PALMRT and a baseline method, plotted against the targeted F-test absolute power for various signal sizes. Different colors indicate varying feature dimensions p .

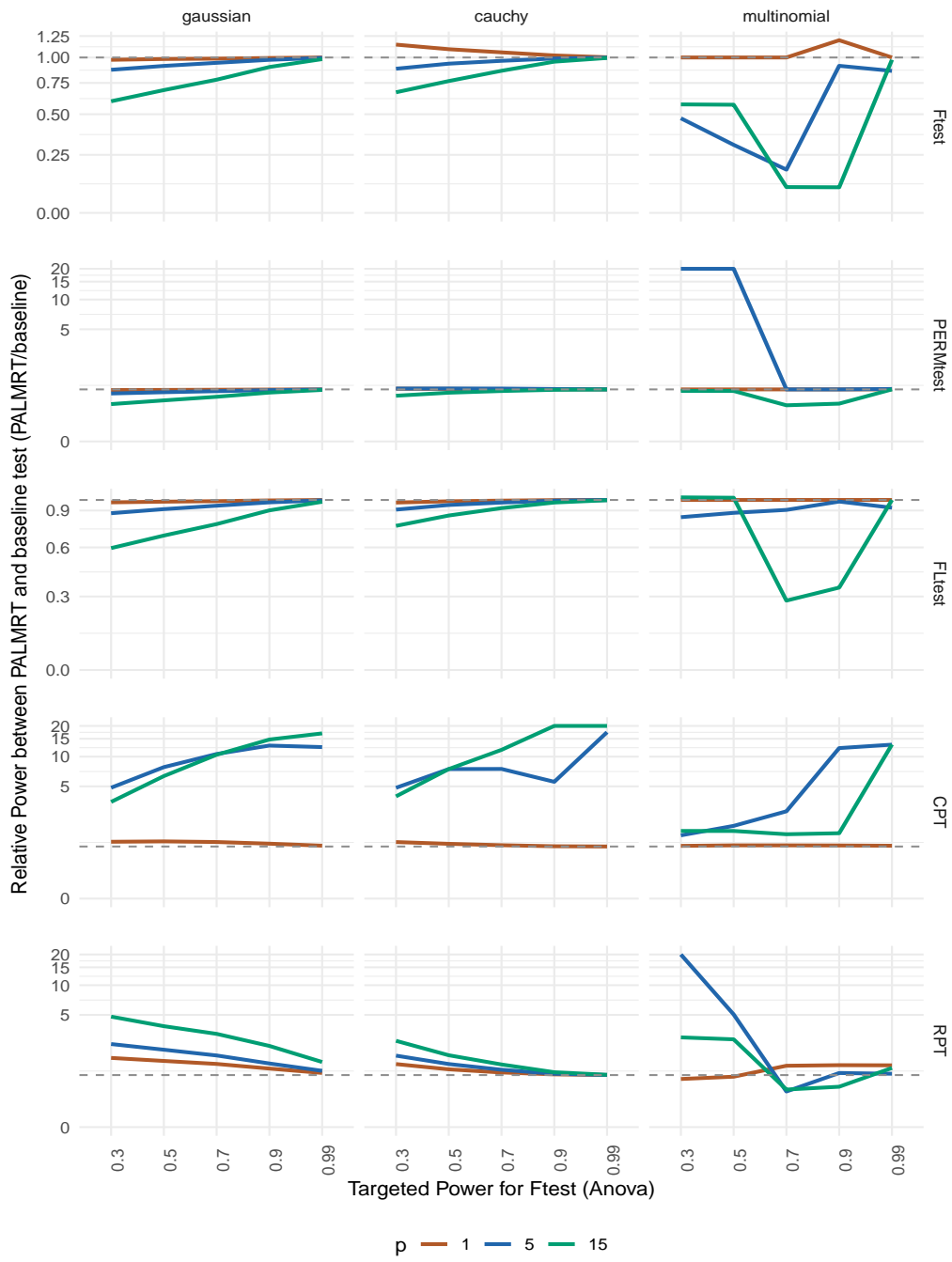


Figure 5: Power analysis in Anova design, presented as line plots, organized by baseline methods (row names) and noise distributions (column names). Each line plot shows the median power ratio between PALMRT and a baseline method, plotted against the targeted F-test absolute power for various signal sizes. Different colors indicate varying feature dimensions p .

Overall, PALMRT has consistently higher power than CPT in the Gaussian, Cauchy, and ANOVA designs, despite becoming more conservative as p increases, and is also more powerful than RPT. When (n/p) is large, PALMRT and FLtest perform similarly, but their relative diverges as (n/p) decreases. This divergence is contingent on both design and noise distributions.

6.3 Coverage evaluation of CI_α

In this section, we evaluate the empirical coverage and median length of confidence intervals (CI_α) constructed using Algorithm 2 (“Inversion”), Bootstrap, and normal approximation (“Normal”) across Gaussian, Cauchy, and Anova designs for various β . We exclude the Paired design due to undefined Bootstrap CIs for all p . As CI coverage and length are consistent across different β , for the sake of space, we focus on results with a targeted F-test power of 50% and defer full results to the supplementary materials.

Figure 6A presents the achieved coverage. The CIs from Inversion consistently meet the desired coverage. In contrast, the normal CIs exhibit slight under-coverage in the ANOVA design with Cauchy noise, and Bootstrap CIs show severe under-coverage for Cauchy noise. For the ANOVA design with $p = 15$, Bootstrap CIs are undefined and thus omitted in Figure 6A. Figure 6B shows the median CI lengths for each method. In line with previous findings, CIs from Algorithm 2 are generally wider than Normal CIs, except for $p = 1$ with Cauchy noise. Bootstrap CIs can exhibit greater variability when the designs are dominated by extreme values, such as in the Cauchy design setting.

7 Robust Identification of long-Covid biomarkers

The MY-LC dataset contains measurements of 64 cell frequencies for 101 long-Covid (LC) participants and 84 controls (42 healthy samples, 42 convalescent samples without LC). A small percentage of measures are missing, with the number of observed samples ranging from 169 to 177 across features. Significant partial correlations between LC status and cell frequencies were identified by Klein et al. (2023), after controlling for age, sex, and BMI as described in eq. (2). Among the 64 features, 26 had $p \leq 0.05$, and 5 survived multiple hypothesis correction using the BH procedure. In this work, we apply PALMRT, CPT, and RPT, which are theoretically guaranteed and validated through simulations, for robust biomarker identification.

Figure 7A displays confidence intervals generated using Algorithm 2 for the 26 significant biomarkers identified by the t-test, before multiple corrections, at $\alpha = 0.05$.

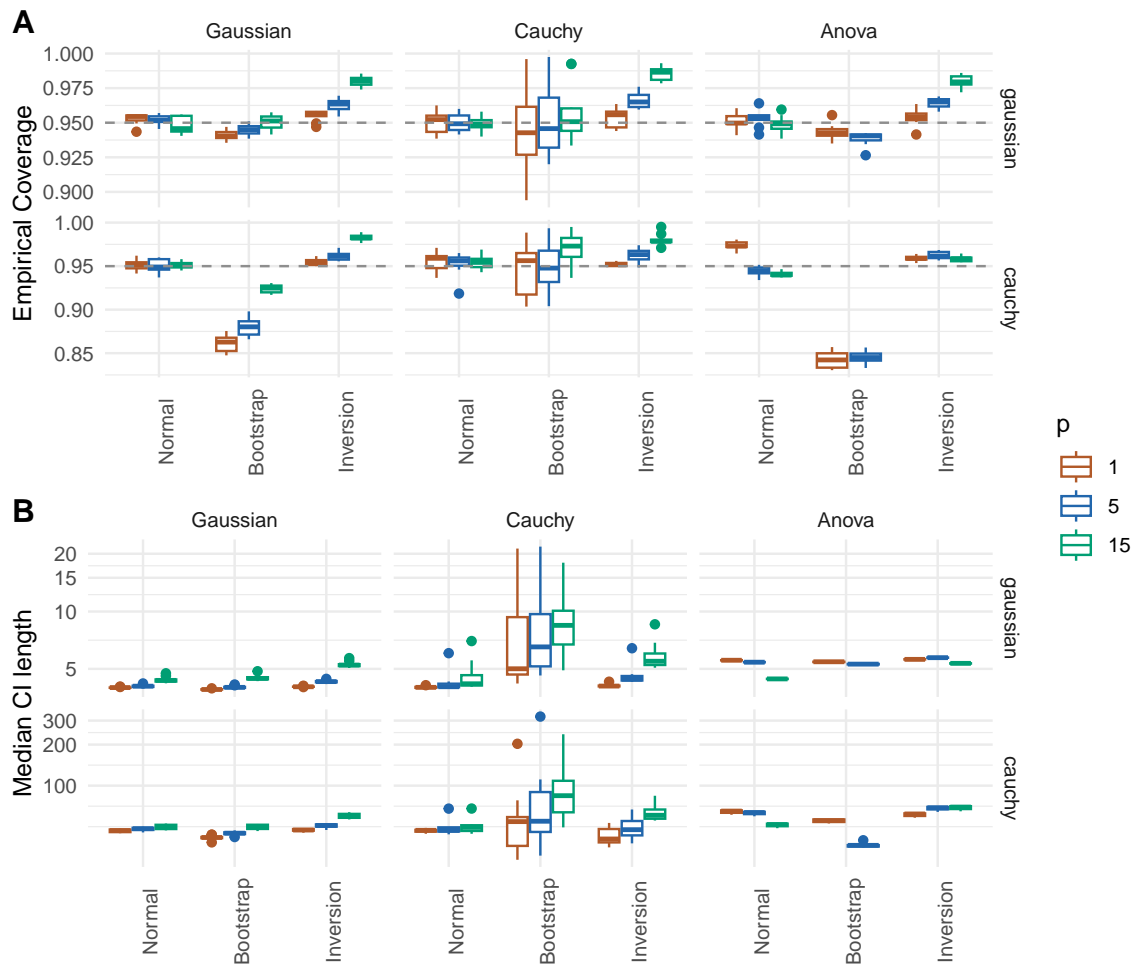


Figure 6: CI coverage and length comparisons, presented as boxplots, organized by designs (row names) and noise distributions (column names). Panel A displays the boxplots of coverage (y-axis) for different CI construction methods (x-axis). Panel B shows the boxplots of median CI length (y-axis) for different CI construction methods (x-axis). Both panels are colored by the feature dimension p .

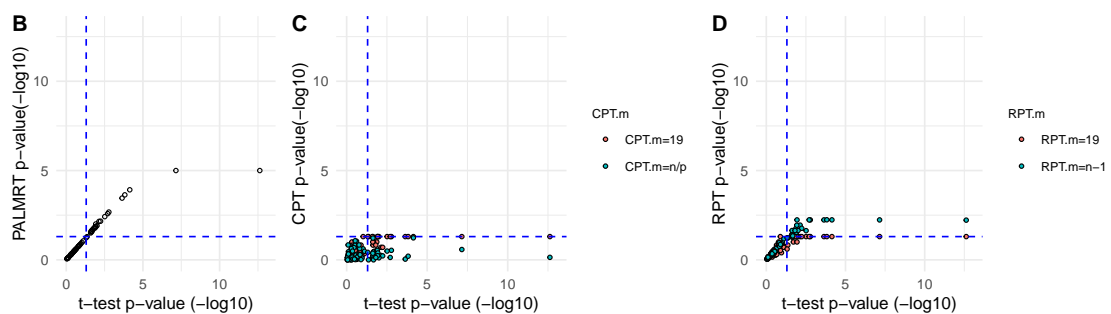
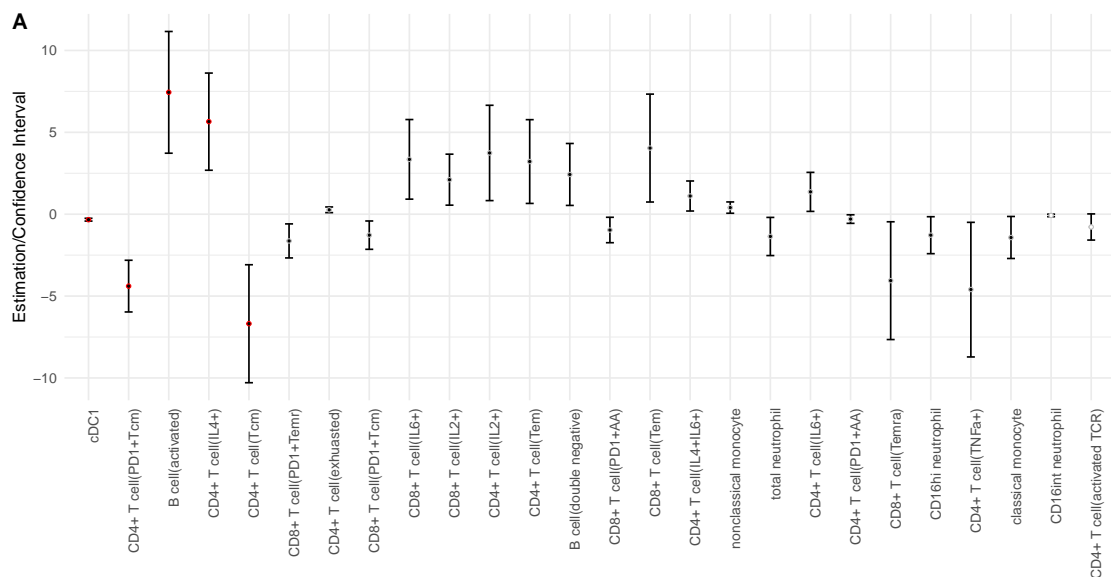


Figure 7: Biomarker discovery using PALMRT and CPT. Panel A displays the estimated coefficient (center dot) and constructed CI (segmented line) for PALMRT for the 26 significant t-test findings before correction, with the x-axis label showing the feature name (ordered based on significance). The center dot is solid if $p\text{-value} \leq \alpha$ and empty otherwise using PALMRT. If a feature is significant after correction using PALMRT, the center dot is further highlighted with red circle. Panel B shows the negative log10 of the PALMRT p-value against that from the t-test for 64 features. Panel C shows the negative log10 of the CPT p-value against that from the t-test for 64 features, where a dot is colored red if CPT used $m = 19$ (CPT.m= 19) and blue if CPT used $m = \lfloor \frac{n}{p} \rfloor - 1$ (CPT.m= n/p). Panel D shows the negative log10 of the RPT p-value against that from the t-test for 64 features, where a dot is colored red if RPT used $m = 19$ (RPT.m= 19) and blue if RPT used $m = n - 1$ (RPT.m= $n - 1$). The vertical/horizontal dashed lines represent the p-value level of 0.05 in Panels B-D.

The center dot in each CI represents the estimated LC coefficient in eq. (2). Solid dots indicate features that were significant before correction; empty dots indicate otherwise. PALMRT confirmed 24 of these 26 biomarkers. In particular, all 5 top biomarkers, which were significant after correction using the t-test, remained significant after correction using PALMRT (solid dot with red circle). In general, the p-values from PALMRT and the t-test are highly concordant, with ratios between them for the same feature ranging from 0.6 to 1.2, except for cDC1 and the central memory CD4+ T cell with positive PD1 (CD4+ T cell (PD1+Tcm)), which achieved the smallest possible PALMRT p-values at $B = 10^5$ and also had smallest t-test p-values $\ll 10^{-5}$ (see Figure 7B).

Both CPT and RPT, in contrast, reduced discoveries before correction and yielded none afterward. Increasing the number of cyclic permutations (m) from $m = 19$ to $m = \lfloor \frac{n}{p} \rfloor - 1$ did not improve their power in CPT, as shown in Figure 7C. The nominal p-value cutoff at 0.05 resulted in 16 out of 26 t-test discoveries being confirmed when $m = 19$ and none being significant when $m = \lfloor \frac{n}{p} \rfloor - 1$ (see Figure 7C). RPT achieved higher power compared to CPT at the nominal p-value cutoff of 0.05, confirming 22 out of 26 t-test discoveries when $m = 19$. However, even for RPT, no discoveries were retained after correcting for multiple hypothesis tests, whether using $m = 19$ or $m = n - 1$, the largest m allowed by the RPT algorithm (see Figure 7D).

8 Discussions

We introduce a novel conformal test, PALMRT, designed for hypothesis testing in linear regression. This test and its corresponding confidence intervals are efficiently computed by evaluating statistic pairs, which are formed by augmenting the original regression problem with row-permuted versions of (x, Z) . PALMRT achieves little power loss compared to conventional tests like the F/t-test and FL-test, and differs from CPT and RPT which also enjoy a worst-case coverage guarantee. Unlike CPT, PALMRT eliminates the need for complex optimization to construct the test and consistently outperforms CPT in both simulated and real-data scenarios. In comparison to RPT, another recently proposed method, developed independently to address the challenges in CPT, PALMRT does not require specially designed permutations that form a group, and its performance remains stable and does not deteriorate as the number of permutations increases.

Of note, the improvement over CPT is not universal. For example, in special designs like the paired design where there are many duplicate rows in Z , CPT can be more powerful. Figure 8 illustrates the comparative power of CPT and PALMRT

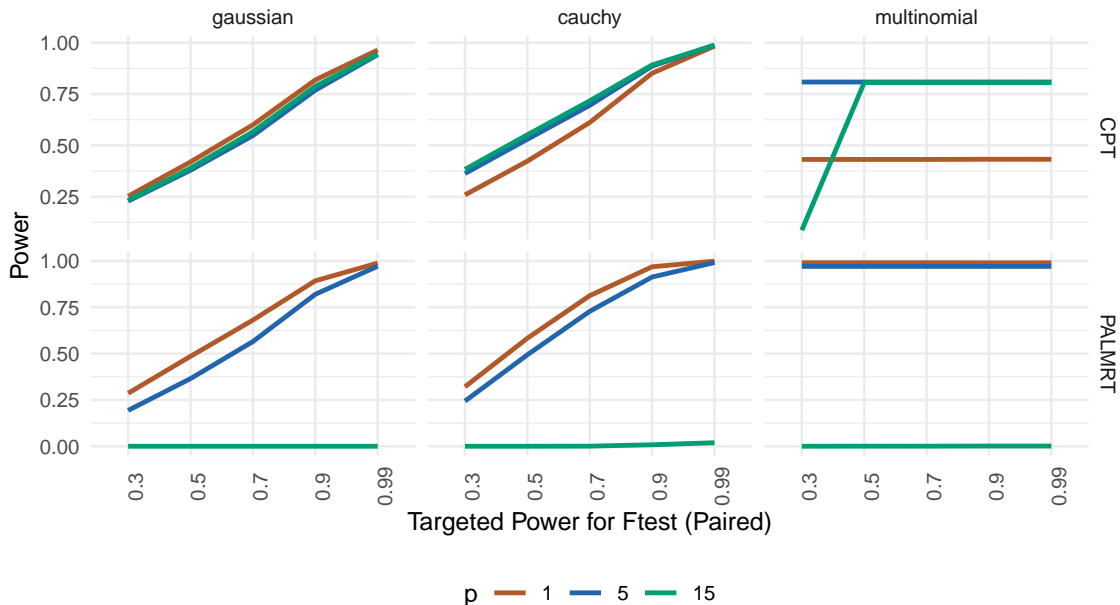


Figure 8: Power analysis in Anova design, presented as line plots, organized by methods (row names) and noise distributions (column names). Each line plot shows the median power of a given method and dimension p , plotted against the targeted F-test power for various signal sizes. Different colors indicate varying feature dimensions p .

in signal detection under the paired design. While PALMRT generally matches or exceeds the power of CPT when $p = 1, 5$, it fails to detect signals at $\alpha = 0.05$ when $p = 15$. CPT, conversely, successfully identifies an effective pre-ordering and η to construct a non-trivial test. While such settings are rare in practice, this observation raises an intriguing theoretical inquiry: Can the power of PALMRT be enhanced by filtering the random permutations $\{x_{\pi_b}, Z_{\pi_b}\}$ to avoid near co-linearity among $x, Z, x_{\pi_b}, Z_{\pi_b}$? We earmark this question for future exploration.

As a brief detour from our main discussion, the augmentation step in PALMRT is reminiscent of the seminal work by Barber and Candès (2015), which introduced the concept of knockoffs. This approach generates a knockoff copy \tilde{X} of the original feature matrix X , e.g., $X \leftarrow (x, Z)$ in our notation with dimension $n \times (p + 1)$. The key requirement of the knockoff copy is that swapping any pair (\tilde{X}_j, X_j) leaves the covariance structure unchanged. Consequently, important quantities in regression analysis—such as OLS or Lasso coefficients $(\hat{\beta}_1, \dots, \hat{\beta}_{p+1}, \tilde{\beta}_1, \dots, \tilde{\beta}_{p+1})$ —are invariant

under these swaps, provided the error terms $\varepsilon_1, \dots, \varepsilon_n$ are i.i.d Gaussian. Knockoffs control the FDR by retaining features X_j for which $|\hat{\beta}_j| - |\tilde{\beta}_j|$ is sufficiently large. Although both PALMRT and knockoffs operate under a fixed design and have similar sample size requirements, their objectives differ. Knockoffs aim to control FDR across $p + 1$ features under the Gaussian noise assumption, often in more complex model-fitting contexts, whereas PALMRT focuses on computing individual p-values for partial correlations under a more relaxed exchangeability condition for the residual errors. Recent advancements in derandomized knockoffs (Ren and Barber, 2022) allow for the computation of modified e-values (Vovk and Wang, 2021; Wang and Ramdas, 2022) through repeated runs with different \tilde{X} copies. However, achieving small p-values or high e-values necessitates a large $n > \text{e-value}$ or $n > (1/\text{p-value})$ at least, a constraint not shared by PALMRT. This makes PALMRT particularly advantageous for exploratory analyses aimed at uncovering partial correlations among a potentially large set of response and primary feature pairs, after adjusting for a limited number of covariates.

Acknowledgment

The author would like to thank Dr. Akiko Iwasaki and her team for providing access to the MY-LC data.

Funding

L.G. was supported in part by the NSF award DMS2310836.

References

- Anderson, M. J. and J. Robinson (2001). Permutation tests for linear models. *Australian & New Zealand Journal of Statistics* 43(1), 75–88.
- Barber, R. F. and E. J. Candès (2015). Controlling the false discovery rate via knockoffs. *The Annals of Statistics* 43(5).
- Barber, R. F., E. J. Candès, A. Ramdas, and R. J. Tibshirani (2021). Predictive inference with the jackknife+.

- Davison, A. C. and D. V. Hinkley (1997). *Bootstrap methods and their application*. Number 1. Cambridge university press.
- DiCiccio, T. J. and B. Efron (1996). Bootstrap confidence intervals. *Statistical science* 11(3), 189–228.
- DiCiccio, T. J. and J. P. Romano (1988). A review of bootstrap confidence intervals. *Journal of the Royal Statistical Society Series B: Statistical Methodology* 50(3), 338–354.
- Draper, N. R. and D. M. Stoneman (1966). Testing for the inclusion of variables in linear regression by a randomisation technique. *Technometrics* 8(4), 695–699.
- Edgington, E. and P. Onghena (2007). *Randomization tests*. CRC press.
- Efron, B. (1987). Better bootstrap confidence intervals. *Journal of the American statistical Association* 82(397), 171–185.
- Efron, B. and B. Narasimhan (2020). The automatic construction of bootstrap confidence intervals. *Journal of Computational and Graphical Statistics* 29(3), 608–619.
- Efron, B. and R. J. Tibshirani (1994). *An introduction to the bootstrap*. CRC press.
- Fisher, R. A. (1922). The goodness of fit of regression formulae, and the distribution of regression coefficients. *Journal of the Royal Statistical Society* 85(4), 597–612.
- Fisher, R. A. (1970). Statistical methods for research workers. In *Breakthroughs in statistics: Methodology and distribution*, pp. 66–70. Springer.
- Fisher, R. A. et al. (1924). 036: On a distribution yielding the error functions of several well known statistics.
- Freedman, D. and D. Lane (1983). A nonstochastic interpretation of reported significance levels. *Journal of Business & Economic Statistics* 1(4), 292–298.
- Garthwaite, P. H. (1996). Confidence intervals from randomization tests. *Biometrics*, 1387–1393.
- Gupta, C., A. K. Kuchibhotla, and A. Ramdas (2022). Nested conformal prediction and quantile out-of-bag ensemble methods. *Pattern Recognition* 127, 108496.

- Hall, P. (1988). Theoretical comparison of bootstrap confidence intervals. *The Annals of Statistics*, 927–953.
- Hall, P. and S. R. Wilson (1991). Two guidelines for bootstrap hypothesis testing. *Biometrics*, 757–762.
- Han, Y., M. Xu, and L. Guan (2023). Conformalized semi-supervised random forest for classification and abnormality detection. *arXiv preprint arXiv:2302.02237*.
- Kennedy, F. E. (1995). Randomization tests in econometrics. *Journal of Business & Economic Statistics* 13(1), 85–94.
- Kim, B., C. Xu, and R. Barber (2020). Predictive inference is free with the jackknife+-after-bootstrap. *Advances in Neural Information Processing Systems* 33, 4138–4149.
- Klein, J., J. Wood, J. Jaycox, R. M. Dhodapkar, P. Lu, J. R. Gehlhausen, A. Tabachnikova, K. Greene, L. Tabacof, A. A. Malik, et al. (2023). Distinguishing features of long covid identified through immune profiling. *Nature*, 1–3.
- Lei, L. and P. J. Bickel (2021). An assumption-free exact test for fixed-design linear models with exchangeable errors. *Biometrika* 108(2), 397–412.
- Manly, B. F. (2006). *Randomization, bootstrap and Monte Carlo methods in biology*, Volume 70. CRC press.
- Meinshausen, N. (2015). Group bound: confidence intervals for groups of variables in sparse high dimensional regression without assumptions on the design. *Journal of the Royal Statistical Society Series B: Statistical Methodology* 77(5), 923–945.
- Pitman, E. J. G. (1937). Significance tests which may be applied to samples from any populations. ii. the correlation coefficient test. *Supplement to the Journal of the Royal Statistical Society* 4(2), 225–232.
- Ren, Z. and R. F. Barber (2022). Derandomized knockoffs: leveraging e-values for false discovery rate control. *arXiv preprint arXiv:2205.15461*.
- Ter Braak, C. J. (1992). Permutation versus bootstrap significance tests in multiple regression and anova. In *Bootstrapping and Related Techniques: Proceedings of an International Conference, Held in Trier, FRG, June 4–8, 1990*, pp. 79–85. Springer.

- Vovk, V., I. Nouretdinov, V. Manokhin, and A. Gammerman (2018). Cross-conformal predictive distributions. In *conformal and probabilistic prediction and applications*, pp. 37–51. PMLR.
- Vovk, V. and R. Wang (2021). E-values: Calibration, combination and applications. *The Annals of Statistics* 49(3), 1736–1754.
- Wang, R. and A. Ramdas (2022). False discovery rate control with e-values. *Journal of the Royal Statistical Society Series B: Statistical Methodology* 84(3), 822–852.
- Wen, K., T. Wang, and Y. Wang (2022). Residual permutation test for high-dimensional regression coefficient testing. *arXiv preprint arXiv:2211.16182*.
- Westfall, P. H. and S. S. Young (1993). *Resampling-based multiple testing: Examples and methods for p-value adjustment*, Volume 279. John Wiley & Sons.
- Winkler, A. M., G. R. Ridgway, M. A. Webster, S. M. Smith, and T. E. Nichols (2014). Permutation inference for the general linear model. *Neuroimage* 92, 381–397.

A Proofs

A.1 Proof of Lemma 4.3

Proof. Recall that $T_{0b}(\beta) = \|(I - H^{x_{\pi_b} z_{\pi_b} z})(y - x\beta)\|_2^2$ and $T_{b0}(\beta) = \|(I - H^{x z z \pi})(y - x\beta)\|_2^2 = \|(I - H^{x z z \pi})y\|_2^2 = c_{b4}$. Hence, $T_{b0}(\beta)$ does not depend on β , and we only need to examine how β influences $T_{0b}(\beta)$. When x lies in the space spanned by $(z, z_{\pi_b}, x_{\pi_b})$, we have $c_{b1} = 0$, and

$$\begin{aligned} T_{0b}(\beta) &= \|(I - H^{x_{\pi_b} z z \pi_b})(y - x\beta)\|_2^2 \\ &= \|(I - H^{x_{\pi_b} z \pi_b})y\|_2^2 \\ &= \|(I - H^{x_{\pi_b} z \pi_b z})y\|_2^2 = c_{b3}. \end{aligned}$$

Hence, when $c_{b3} = c_{b4}$, we have $\omega_b(\beta) = 1/2$ and when $c_{b3} < c_{b4}$, we have $\omega_b(\beta) = 1$.

When x does not lie in the space spanned by $(z, z_{\pi_b}, x_{\pi_b})$, we have, $c_{b1} > 0$, and

$$\begin{aligned} T_{0b} \leq T_{b0} &\Leftrightarrow \|(I - H^{x_{\pi_b} z \pi_b z})(y - x\beta)\|_2^2 \leq c_{b4}, \\ &\Leftrightarrow c_{b1}\beta^2 - 2c_{b2}\beta + (c_{b3} - c_{b4}) \leq 0, \end{aligned}$$

$$\Rightarrow s_b := \frac{c_{b2} - \sqrt{c_{b2}^2 - c_{b1}(c_{b3} - c_{b4})}}{a_{b1}} \leq \beta \leq u_b := \frac{c_{b2} + \sqrt{c_{b2}^2 - c_{b1}(c_{b3} - c_{b4})}}{a_{b1}}.$$

Note that we must have $c_{b2}^2 \geq c_{b1}(c_{b3} - c_{b4})$, and consequently, real-valued solutions $s_b \leq u_b$ exist. This follows from the following argument.

Set β as the OLS coefficient estimate for x in the regression $y \sim x + Z + x_\pi + Z_\pi$. We have

$$\begin{aligned} T_{0b} &= \|(I - H^{x_{\pi_b} z_{\pi_b} z})(y - x\beta)\|_2^2 \\ &= \|(I - H^{x z x_{\pi_b} z_{\pi_b}})y\|_2^2 \\ &= \|(I - H^{R^{x_{\pi_b} | x z z_{\pi_b}}})(I - H^{x z z_{\pi_b}})y\|_2^2 \\ &\leq \|(I - H^{x z z_{\pi_b}})y\|_2^2 = T_{b0}. \end{aligned}$$

Here, we use $R^{x_{\pi_b} | z_{\pi_b} x z}$ to denote the regression residuals of x_{π_b} in the regression $x_\pi \sim Z + x + Z_\pi$. Hence, the previous quadratic function is guaranteed to have real-valued root(s) when $c_{b1} > 0$. \square

A.2 Proof of Theorem 4.4

Utilizing Lemma 4.3, we know that value β satisfies $f(\beta) := \frac{1 + \sum_{b=1}^B \omega_b(\beta)}{B+1} > \alpha$ if and only if

$$f_{A_1}(\beta) := \sum_{b \in A_1} \omega_b(\beta) > \gamma := (B+1)\alpha - |A_2| - \frac{1}{2}|A_3| - 1,$$

where $A_1 = \{b : c_{b1} > 0\}$, $A_2 = \{b : c_{b1} = 0, c_{b3} < c_{b4}\}$, and $A_3 = \{b : c_{b1} = 0, c_{b3} = c_{b4}\}$; $\omega_b(\beta) = \frac{1}{2}\mathbb{1}\{s_b \leq \beta \leq u_b\} + \frac{1}{2}\mathbb{1}\{s_b < \beta < u_b\}$ for $b \in A_1$. We can rearrange $\omega_b(\beta)$ for $b \in A_1$:

$$\omega_b(\beta) = \frac{1}{2}(\mathbb{1}\{\beta \geq s_b\} + \mathbb{1}\{\beta > s_b\} - \mathbb{1}\{\beta \geq u_b\} - \mathbb{1}\{\beta > u_b\}). \quad (12)$$

Summing over all terms $b \in A_1$, we obtain that

$$\begin{aligned} f_{A_1}(\beta) &= \frac{1}{2} \left(\sum_{b \in A_1} \mathbb{1}\{\beta \geq s_b\} + \sum_{b \in A_1} \mathbb{1}\{\beta > s_b\} - \sum_{b \in A_1} \mathbb{1}\{\beta \geq u_b\} - \sum_{b \in A_1} \mathbb{1}\{\beta > u_b\} \right) \\ &= \frac{1}{2} (\#\{b : s_b \leq \beta\} + \#\{b : s_b < \beta\} - \#\{b : u_b \leq \beta\} - \#\{b : u_b < \beta\}). \end{aligned} \quad (13)$$

The function $f_{A_1}(\beta) \geq 0$ is a piece-wise constant function with change points being $t_1 < \dots < t_M$. Hence, when $\gamma < 0$, $f_A(\beta) > \gamma$ is guaranteed.

When $\gamma \geq 0$, we must have $t_1 \leq \beta < t_M$ in order to have $f_A(\beta) > \gamma$ since $f(\beta) = 0$ for $\beta < t_1$ and $\beta \geq t_M$. It is obvious that for $\beta = t_1$, $f_A(\beta) = \frac{1}{2}(m_1^s - m_1^u)$. Suppose we know $f_A(t_l)$. Then,

- Increasing β from t_l to a value in (t_l, t_{l+1}) : For all $\beta \in (t_l, t_{l+1})$, because for those s_b, u_b smaller than t_l or those no smaller than t_{l+1} , their contributions will not change in eq. (13), and only those at exactly at t_l will add contribution $1/2$ or $-1/2$ as the corresponding comparisons to t_l change from equality to inequality. Hence, we have

$$f(\beta) = f_A(t_l) + \frac{1}{2}(m_l^s - m_l^u), \quad \forall \beta \in (t_l, t_{l+1}).$$

We denote this function value as $f(t_l^+)$ to indicate being in the open interval (t_l, t_{l+1}) .

- Increasing β from a value in (t_l, t_{l+1}) to t_{l+1} : For those s_b, u_b no greater than t_l or those greater than t_{l+1} , their contributions will not change in eq. (13), and only those who now hit t_{l+1} exactly will add contribution $1/2$ or $-1/2$ for newly satisfied comparisons to t_{l+1} . Hence, we have

$$f(t_{l+1}) = f_A(t_l^+) + \frac{1}{2}(m_{l+1}^s - m_{l+1}^u).$$

These confirms our induction rule described in the main paper. Finally,

- The smallest value of β at the critical values $\{t_l\}_{l=1}^M$ that satisfies $f_A(t_l) > \gamma$ is $\min\{t_l : f_A(t_l) > \gamma\}$. The smallest interval (t_l, t_{l+1}) that satisfies $f_A(\beta) > \gamma$ for $\beta \in (t_l, t_{l+1})$ is $\min\{(t_l, t_{l+1}) : f_A(t_l^+) > \gamma\}$, which leads to infimum value $\min\{t_l : f_A(t_l^+) > \gamma\}$. Hence, $\beta_{\min} = \min\{t_l : f_A(t_l) \vee f_A(t_l^+) > \gamma\}$.
- The largest value of β at the critical values $\{t_l\}_{l=1}^M$ that satisfies $f_A(t_l) > \gamma$ is $\max\{t_l : f_A(t_l) > \gamma\}$. The largest interval (t_l, t_{l+1}) that satisfies $f_A(\beta) > \gamma$ for $\beta \in (t_l, t_{l+1})$ is $\max\{(t_l, t_{l+1}) : f_A(t_l^+) > \gamma\}$, which leads to supremum value $\max\{t_l : f_A(t_{l-1}^+) > \gamma\}$. Hence, $\beta_{\max} = \max\{t_l : f_A(t_l) \vee f_A(t_{l-1}^+) > \gamma\}$.

This conclude our proof that Algorithm 2 constructs the exact CI_α described in Lemma 4.3.

B Additional simulation results

B.1 Type I error control at $\alpha = 0.01, 0.001$

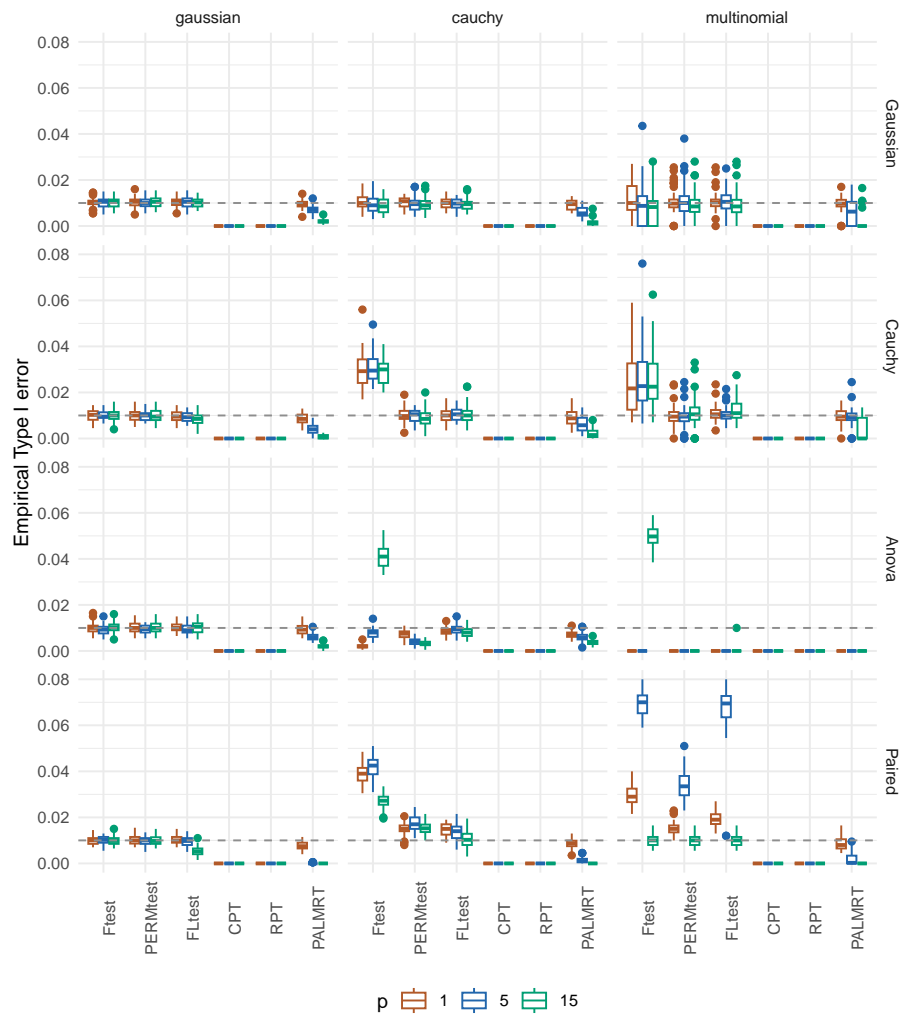


Figure 9: Empirical type I error using various methods, organized into boxplots by corresponding designs (row names) and noise distributions (column names). Each boxplot displays the empirical type I error for different methods, separately for different feature dimension p (color). The dashed horizontal line represents the targeted type I error $\alpha = 0.01$.

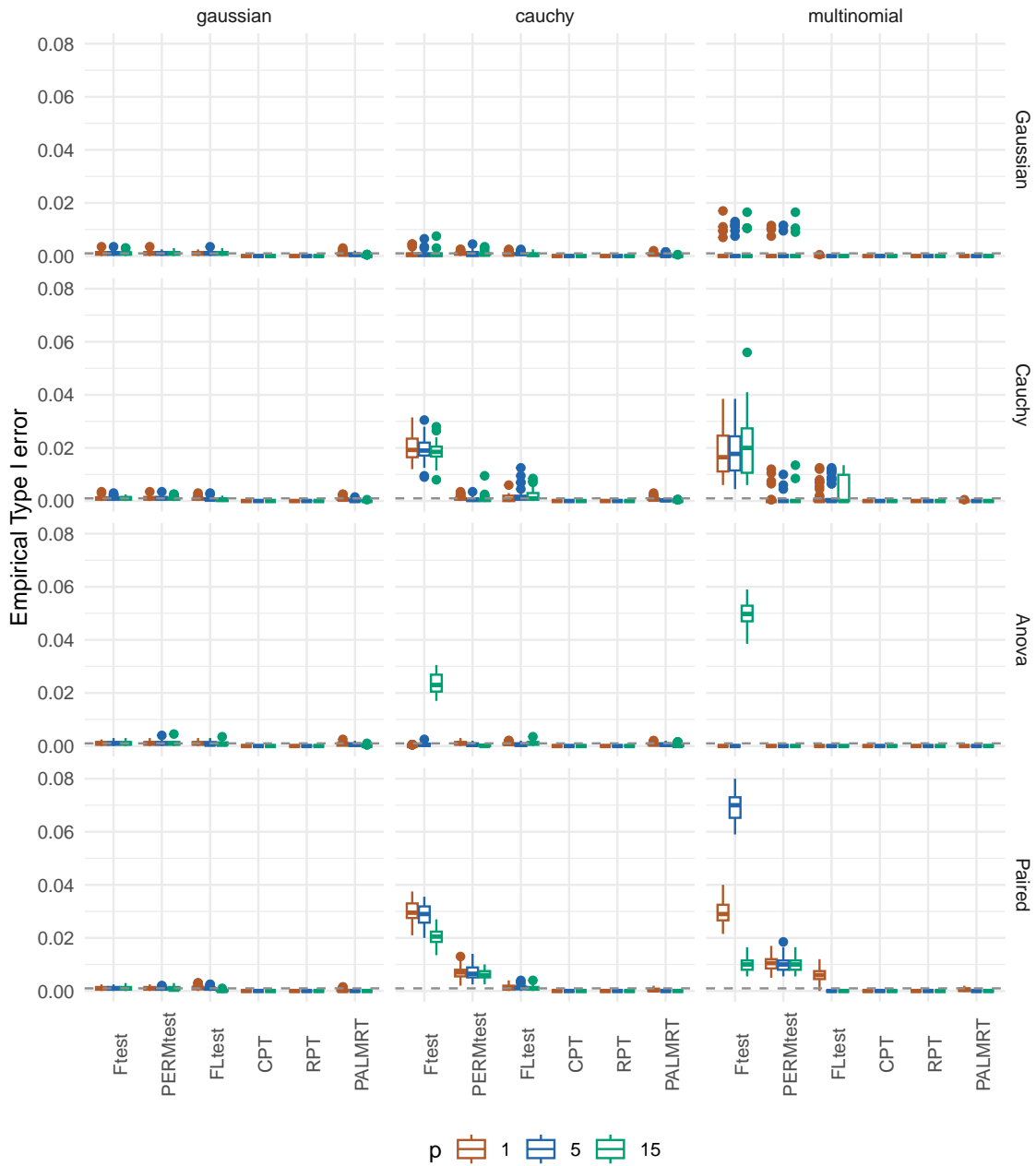


Figure 10: Empirical type I error using various methods, organized into boxplots by corresponding designs (row names) and noise distributions (column names). Each boxplot displays the empirical type I error for different methods, separately for different feature dimension p (color). The dashed horizontal line represents the targeted type I error $\alpha = 0.01$.

B.2 CI coverage with varying signal sizes

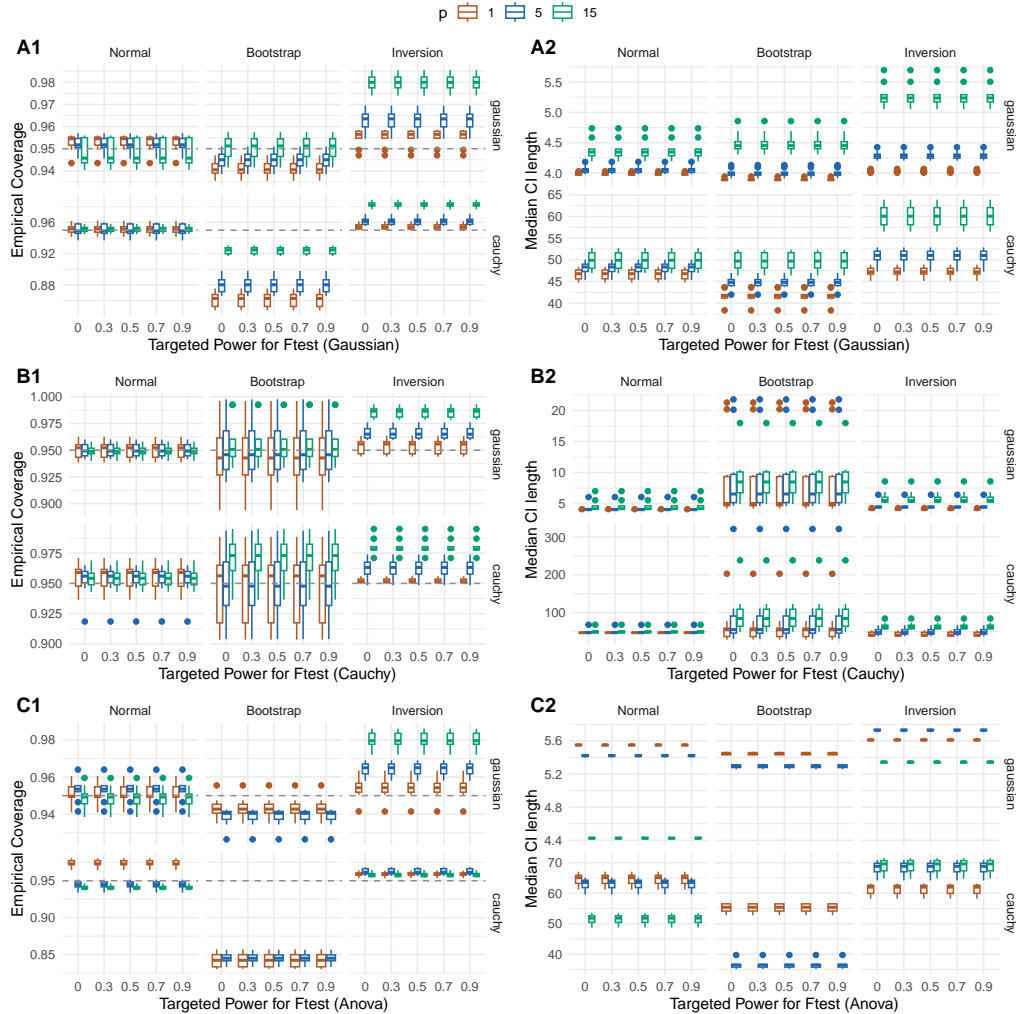


Figure 11: CI coverage and length comparisons, presented as boxplots. Panels A1-C1 display the boxplots of coverage (y-axis) for different signal strength (x-axis) for different designs (indicated in the x-lab label), different noises (row names of a panel), methods (column names of a panel), and feature dimension p (color). Panels A2-C3 display the boxplots of CI's median length (y-axis) for different signal strength (x-axis) for different designs (indicated in the x-lab label), different noises (row names of a panel), methods (column names of a panel), and feature dimension p (color).